Tools and Insights for Sustainable Management of Plant Pests and Pathogens

by

Noah Bevers

A thesis submitted to the Graduate Faculty of
Auburn University
in partial fulfillment of the
requirements for the Degree of
Master of Science

Auburn, Alabama
May 7, 2022

soybean diseases, convolutional neural networks, computer vision,
plant pathogens, virulence evolution, disease diagnostics

Approved by

Dr. Nate B. Hardy, Chair, Associate Professor, Entomology & Plant Pathology
Dr. Edward J. Sikora, Extension Special Professor, Entomology & Plant Pathology
Dr. Alana L. Jacobson, Associate Professor, Entomology & Plant Pathology

Thesis Abstract

Minimizing crop yield losses caused by plant pathogens is one way of increasing agricultural productivity. To that end, I developed an automated classifier of digital images of soybean diseases to assist with early and accurate detection of pathogens. This application, based on a convolutional neural network, distinguishes between eight soybean disease/deficiency classes with an overall accuracy of 96.75%, which may help minimize pesticide usage and improve overall productivity. I also performed a quantitative integration of the existing research characterizing the relationship between virulence and within-host pathogen accumulation. By doing so, I aimed to help increase our ability to foresee and manage the evolution of highly-virulent pathogen genotypes. In these two ways, I pursued my overarching goal of developing tools and gaining insights for the sustainable management of plant pathogens.

Table of Contents

List of Tables

List of Figures

Chapter I: Background

Introduction and Problem Statement

Agronomic crops are cultivated for an expanding assortment of usages such as food, fiber, oil, fuel, medicine, recreation, ecosystem conservation, and other industrial applications (Naz et al. 2019). Maintaining food security and meeting the demands for bio-materials from an expected growing human population (Hofstra and Vermeulen 2016) is a constantly evolving challenge that will require a dynamic and diverse set of solutions from multiple sectors. In recent decades, the global area of cultivated land has been increasing to meet the demand for agricultural materials (Frona et al. 2019), but it is uncertain how long this practice can be soundly continued. Moreover, this demand needs to be balanced against the need to conserve natural resources and natural ecosystem functions (Mehrabi et al. 2018). Ultimately, there is a limit to just how much land can be allocated to agriculture, and in some areas there is already fierce competition (Frona et al. 2019). To keep pace with current global consumption trends, agricultural yields need to increase at a rate higher than that of population growth while also minimizing negative environmental or socio-economic impacts (Frona et al. 2019). Without increasing the area of land for farming, production gains depend on increases in productivity (Kalaitzandonakes et al. 2019).

One way of increasing productivity is to minimize production losses caused by pests and pathogens. This is the overarching goal of my thesis research; I sought to develop tools and gain insights that could promote sustainable management of the pests and pathogens of plants. In pursuit of this broad goal, I performed two specific research projects: I explored the possibility of

using artificial intelligence to make it easier to diagnose diseases of soybeans, and I performed a quantitative integration of the existing research to get a clearer picture of the nature of virulence evolution in plant pathosystems. Before we turn to those specific projects, let us first consider in more detail the challenges that pests and pathogens pose for sustainable agriculture.

Agricultural Challenges: Pests and Pathogens

The large monoculture-heavy farms that predominate today are particularly vulnerable to outbreaks of pests and pathogens (Zadoks and Schein 1979, Bebber et al. 2019, Savary et al. 2019a). Furthermore, the expanding connectedness of global trade brings increased risk of rapid pest and pathogen emergences as former natural migration boundaries are dissolved (Savary et al. 2019b). And, as climate changes, so will the favorable environmental conditions for crop pathogens and pests as their latitudinal ranges are expected to shift (Chaloner et al. 2021). It is estimated that most countries currently only report approximately 20% of the pests that could theoretically be supported based on available host plants (Bebber et al. 2014). This allows a lot of room for invasion by potential pests and underscores the importance of quickly identifying and controlling newcomers. Microbial pathogens can be particularly difficult to notice upon inspection and the detection of plant pests may lag behind their establishment within a country or region by several years (Poland and Mccullough 2005, Liebhold and Tobin 2006, Eschen et al. 2019). For example, it is predicted that there are extensive but unrecognized pest faunas in China, India, Brazil, and Russia (Bebber et al. 2019). In summary, as our farms have become larger and more uniform, they have also become more vulnerable to pest outbreaks, and as our economies have become more globalized and connected, the total pest pressure on our farms has

increased. Simply put, the risk posed by pests and plant diseases in agriculture has never been greater.

Pests and pathogens cost billions of dollars in crop losses every year (Fried et al. 2017). Research focusing on five major crops – wheat, rice, maize, potato, and soybean – found that pests and pathogens caused global crop losses between 17 and 23% for all crops except for rice, which was closer to 30% (Savary et al. 2019b). Combined, these five crops contribute approximately 48.1% of the global human calorie consumption (2013 estimates) (Savary et al. 2019b, *FAOSTAT* 2021). Pests and pathogens can directly damage plant tissues making them largely unusable, inedible, or unmarketable. They can also reduce yield by competing with crops for limited environmental resources such as sun light, water, nutrients, and space (Fried et al. 2017). Overall, pests and pathogens can cause an average estimated crop yield reduction of 10-40% (Fried et al. 2017). To reiterate, every unit of crop production can be vital, especially in regions with high levels of food insecurity. Growing populations need reliable access to food and fiber.

Pesticide Usage

In the recent past, crop losses due to pests and pathogens have largely been mitigated by the economical usage of pesticides (Fried et al. 2017). Pesticides have proven to be an effective way to kill insects, pests, pathogens, and weeds and to enhance crop yield and quality (Sharma et al. 2019, 2020). It's estimated that about one-third of agricultural production depends upon the application of pesticides (Tudi et al. 2021); therefore, they have greatly assisted in keeping the world's population fed, clothed, and sheltered (Sharma et al. 2019, Tudi et al. 2021). Conversely,

yields can be substantially diminished when plants are not protected by pesticides, especially by pathogens with high mobility and environmental flexibility (Fried et al. 2017). Currently, approximately 3 billion kilograms of pesticides are used worldwide each year at a cost of approximately $40 billion USD (Hayes and Hansen 2017, Sharma et al. 2020, Tudi et al. 2021).

To reiterate, this extensive use of pesticides has helped to meet the demand for agricultural products, but it has come at a cost to ecosystem and human health (Sharma et al. 2019, 2020). Various pesticides have been reported to have adverse effects on the overall ecosystem including pollution of water sources, contamination of soils, volatilization into the atmosphere, and causing toxicity to non-target plants and organisms (Hayes and Hansen 2017, Sharma et al. 2019, 2020, Hashimi et al. 2020, Tudi et al. 2021). Chemical residues on food and in the environment also raise concerns regarding the harmful effects on human health (Nicolopoulou-Stamati et al. 2016, Abolhassani et al. 2019, Hashimi et al. 2020, Sharma et al. 2020). Putting these concerns aside, the heavy use of pesticides also poses challenges for sustainability. The continuous use of pesticides favors the development of resistance among pests and ultimately, renders these chemical compounds ineffective (Fried et al. 2017, Sharma et al. 2020).

Pesticides play a large and important role in our agricultural systems, but their adverse consequences and their overall effectiveness is best maintained when we do not over rely upon them. Developing tools and theory to help use pesticides more strategically will be key for more sustainable integrated pest management strategies.

Soybean Pests and Pathogens

One of my thesis chapters focuses on the development of more efficient disease diagnostics in soybean. Here, I provide some background on the scope of soybean farming, along with a general overview of current soybean pest and pathogen problems.

Soybean (*Glycine max L. Merrill)* is considered one of the five most important global food crops (Savary et al. 2019) and contributes approximately 3.3% of the annual global calories consumed (2013 estimates) (Savary et al. 2019b, *FAOSTAT* 2021). In roughly the last five years, from 2015-2019, there was approximately 21.3 billion bushels of soybeans produced in the United States and Ontario, Canada alone (Bradley et al. 2020). This is an average of approximately $38.3 billion USD each year (Bradley et al. 2020). Nevertheless, much of the crop is lost due to soybean diseases. Diseases may reduce overall yield, but can also reduce the quality of seed (Kalaitzandonakes et al. 2019, Bradley et al. 2020). From 2015 through 2019, it's estimated that soybean losses from the 28 most important pests and pathogens averaged approximately $3.9 billion USD each year (Bradley et al. 2020), with an average loss per acre of $45 USD (Bradley et al. 2020). Overall, the annual average loss of yield in the USA due to soybean diseases is estimated to range between 8 - 25% (Hartman et al. 2016, Savary et al. 2019b, Bradley et al. 2020).

Soybean diseases are caused by a variety of organisms, including bacteria, viruses, plant-parasitic nematodes, and fungi (Bandara et al. 2020, Bradley et al. 2020). Diseases which pose an economic threat vary each season and may depend on several factors such as local environmental conditions, previous disease history, plant variety selections, and farm management

methodologies (Bandara et al. 2020, Bradley et al. 2020). For example, foliar diseases have been reported to have greater impacts on yields in the southern USA as compared to the northern USA (Bradley et al. 2020). Another example, from 2015 to 2019, the fungal disease known as frogeye leaf spot, *Cercospora sojina*, generated more than double the yield loss as compared to the five years prior (Allen et al. 2017, Bradley et al. 2020). Being able to reliably identify and predict the diseases that are present during the growing season can be the difference between profits and losses. For example, consider the introduction of soybean rust into the USA in 2004 (Sikora et al. 2014). Soybean rust is a fungal disease, *Phakopsora pachyrhizi* Sydow, originally reported in Japan, where it is known to reduce yields by as much as half (Pan et al. 2006). In 2003, The disease was destroying 5% of the annual soybean production in Brazil after its introduction in the country in 2003. A similar fate was feared if the disease were to be introduced into the USA (Sikora et al. 2014, Fried et al. 2017). However, upon the arrival of soybean rust in the USA in 2004, a nationwide response that included a disease monitoring program, a coordinated warning system, and preventative education and management were able to mitigate the spread of the disease (Sikora et al. 2014). This is estimated to have saved farmers more than $200 million USD annually when considering unnecessary fungicide usage and minimized chemical exposure in the environment (Hershman et al. 2011, Sikora et al. 2014, Fried et al. 2017). Even with wide-spread success, isolated incidences can still occur. Reported losses from soybean rust of 40-60% in over 500 acres of poorly managed fields in south Alabama in 2012 and 2013 (Sikora et al. 2014). Proper and swift local farm management is key for protecting on-site yields and plays a pivotal role in preventing large-scale or regional outbreaks of disease.

Early detection of disease presence in the field is one of the principal features of good crop management. The earlier a disease is recognized, the stronger of a position a manager will be in to mitigate the disease's effect on yield, as immediate treatments can be made and preventative plans can be put in place, such as using crop rotation or resistant cultivars. Proper and timely identification also helps to minimize any unnecessary pesticide applications and therefore serves to conserve their efficacy by slowing down the development of pesticide resistance. Soybean diseases often present foliar symptoms with distinguishing visual cues such as changes in color, spotting, or development of pustules or lesions. Identifying these diseases upon visual inspection in the field can be quite challenging and in some cases even a professional plant pathologist cannot make a diagnosis without lab work (Miller et al. 2009). For example, sometimes symptoms caused by pathogens are mistaken as herbicide injuries (Bradley et al. 2020). Unfortunately, diagnostic services can be costly for growers as they include third party field scouting, lab work, or consultancy (Bradley et al. 2020). Extending high-accuracy disease diagnostics further into the field by leveraging smartphone and web technologies is a promising approach for democratizing pest management. With this in mind, I set out to develop a computer-aided soybean disease identification tool capable of identifying soybean diseases by using photographs/images taken directly in the farm field.

The details of this research process and the involved model building components are explored in **Chapter 2,** which contains the article prepared for publication entitled "Soybean Disease Identification Using Original Field Images and Transfer Learning with Convolutional Neural Networks".

Virulence Evolution

Developing sustainable management practices for our crop systems will also require a deeper theoretical understanding of the coevolutionary processes between pathogens and their infected host plants. New and unfamiliar virulent host-pathogen interactions are arising more frequently due to increasing global connectedness and a warming climate (Anderson et al. 2020, 2021). For example, the bacterial pathogen, *Xylella fastidiosa,* has a long history of causing disease in a range of American agricultural crops, but recently, in 2013, it was detected in southern Italy causing severe disease and killing many olive trees; some of which have survived since the Roman Empire (Almeida et al. 2019). Since then, variants of the same pathogen have been linked to other emerging disease systems in Europe and elsewhere (Almeida et al. 2019). Other examples include the emergence of new virulent pathogens that have disrupted he production of cavendish banana in Central America, cassava in sub-Saharan Africa, corn in Kenya, and coffee in Central and South America (Anderson et al. 2021). These few examples are far from an exhaustive list and the threat of plant pathogens is vast and constantly changing. The evolution of virulence is of enormous importance to agriculture. We need to thoroughly understand it, so we can better predict and prevent the evolution of new highly-virulent genotypes and populations.

The term virulence refers to the extent to which pathogens harm their host or, more specifically, to the amount of excess mortality caused by infection (D'arcy et al. 2001, Pagan and Garcia-Arenal 2020). A centerpiece of the theoretical work on virulence evolution is the 'virulence-transmission trade-off' hypothesis (Anderson and May 1982, Sacristán and García-Arenal 2008). This hypothesis posits that virulence (harm to the host) is positively linked to within-host

pathogen accumulation (population) and that increases in accumulation will also lead to increases in pathogen transmission by vectors between hosts (Anderson and May 1982, Sacristán and García-Arenal 2008). Pathogen transmission comes at the cost of a shorter infection period; therefore, pathogen virulence involves a fitness 'trade-off' between pathogen accumulation and between-host transmission (Sacristán and García-Arenal 2008). Despite its prevalence in the theoretical work, the available empirical evidence has not been able to confirm or refute the existence of a transmission-virulence trade-off for plant pathogens (Sacristán and García-Arenal 2008, Froissart et al. 2010). To gain clarity regarding the usefulness of the virulence-transmission trade-off hypothesis for plant pathosystems, we analyzed prior experimental studies and performed a meta-analysis testing the assumption of a direct positive relationship between pathogen accumulation and virulence. Further related background and details regarding the meta-analysis can be found in **Chapter 3** which contains the article submitted for publication entitled "Virulence uncorrelated with pathogen accumulation in plants".

Thesis Thumbnail

Meeting the growing demand for agricultural products will require increased production on a limited land area. Focusing on the reduction of yield losses due to pests and pathogens is a straightforward approach to increasing production in our current agricultural systems. I developed an automated classifier of digital images of soybean diseases, based on convolutional neural networks (CNN), to assist with early and accurate detection of pathogens. This may help to minimize pesticide usage and thus boost overall productivity. Furthermore, evolution of virulence in plant pathogens is of great importance to agriculture, so I performed a quantitative integration of the existing research to gain insights into the coevolutionary process. With a

thorough understanding of virulence, we can better predict and prevent the evolution of new highly-virulent genotypes and pathogen populations in our crop systems. Extended throughout my research thesis is the primary goal; to develop tools and gain insights that can promote sustainable management of the pests and pathogens of plants.

References – Chapter I

Abolhassani, M., G. Asadikaram, P. Paydar, H. Fallah, M. Aghaee-Afshar, V. Moazed, H. Akbari, S. D. Moghaddam, and A. Moradi. **2019**. Organochlorine and organophosphorous pesticides may induce colorectal cancer; A case-control study. Ecotoxicol. Environ. Saf. 178: 168–177.

Allen, T. W., C. A. Bradley, A. J. Sisson, E. Byamukama, M. I. Chilvers, C. M. Coker, A. A. Collins, J. P. Damicone, A. E. Dorrance, N. S. Dufault, P. D. Esker, T. R. Faske, L. J. Giesler, A. P. Grybauskas, D. E. Hershman, C. A. Hollier, T. Isakeit, D. J. Jardine, H. M. Kelly, R. C. Kemerait, N. M. Kleczewski, S. R. Koenning, J. E. Kurle, D. K. Malvick, S. G. Markell, H. L. Mehl, D. S. Mueller, J. D. Mueller, R. P. Mulrooney, B. D. Nelson, M. A. Newman, L. Osborne, C. Overstreet, G. B. Padgett, P. M. Phipps, P. P. Price, E. J. Sikora, D. L. Smith, T. N. Spurlock, C. A. Tande, A. U. Tenuta, K. A.Wise, and J. Allen Wrather. **2017**. Soybean yield loss estimates due to diseases in the United States and Ontario, Canada, from 2010 to 2014. Plant Heal. Prog. 18: 19–27.

Almeida, R. P. P., L. De La Fuente, R. Koebnik, J. R. S. Lopes, S. Parnell, and H. Scherm. **2019**. Addressing the New Global Threat of Xylella fastidiosa. Phytopathology. 109: 172–174.

Anderson, K., D. P. Bebber, K. A. Brauman, N. J. Cunniffe, N. V Fedoroff, C. Finegold, K. A. Garrett, A. Gilligan, C. M. Jones, M. D. Martin, K. Macdonald, P. Neenan, A. Records, D. G. Schmale, L. Tateosian, and Q. Wei. **2021**. The persistent threat of emerging plant disease pandemics to global food security. Proc. Natl. Acad. Sci. U. S. A. 118.

Anderson, R., P. E. Bayer, and D. Edwards. **2020**. Climate change and the need for

agricultural adaptation. Curr. Opin. Plant Biol. 56: 197–202.

Anderson, R. M., and R. M. May. **1982**. Coevolution of Hosts and Parasites. Parasitology. 85: 411–426.

Bandara, A. Y., D. K. Weerasooriya, C. A. Bradley, T. W. Allen, and P. D. Esker. **2020**. Dissecting the economic impact of soybean diseases in the United States over two decades. PLoS One. 15: 1–28.

Bebber, D. P., E. Field, H. Gui, P. Mortimer, T. Holmes, and S. J. Gurr. **2019**. Many unreported crop pests and pathogens are probably already present. Glob. Chang. Biol. 25: 2703–2713.

Bebber, D. P., T. Holmes, and S. J. Gurr. **2014**. The global spread of crop pests and pathogens. Glob. Ecol. Biogeogr. 23: 1398–1407.

Bradley, C., T. W. Allen, A. J. Sisson, G. C. Bergstrom, K. M. Bissonnette, J. Bond, E. Byamukama, M. I. Chilvers, A. A. Collins, J. P. Damicone, A. E. Dorrance, N. S. Dufault, P. D. Esker, T. R. Faske, N. M. Fiorellino, L. J. Giesler, G. L. Hartman, C. A. Hollier, T. Isakeit, T. A. Jackson-Ziems, D. J. Jardine, H. M. Kelly, R. C. Kemerait, N. M. Kleczewski, A. M. Koehler, R. J. Kratochvil, J. E. Kurle, D. K. Malvick, S. G. Markell, F. M. Mathew, H. L. Mehl, K. M. Mehl, D. S. Mueller, J. D. Mueller, B. D. Nelson, C. Overstreet, G. B. Padgett, P. P. Price, E. J. Sikora, I. Small, D. L. Smith, T. N. Spurlock, C. A. Tande, D. E. P. Telenko, A. U. Tenuta, L. D. Thiessen, F. Warner, W. J. Wiebold, and K. Wise. **2020**. Soybean yield loss estimates due to diseases in the United States and Ontario, Canada, from 2015 to 2019. Plant Heal. Prog. 21: 238–247.

Chaloner, T. M., S. J. Gurr, and D. P. Bebber. **2021**. Plant pathogen infection risk tracks global crop yields under climate change. Nat. Clim. Chang. 11: 710–715.

D'arcy, C. J., D. M. Eastburn, and G. L. Schumann. **2001**. Illustrated Glossary of Plant Pathology.

Eschen, R., R. O'Hanlon, A. Santini, A. Vannini, A. Roques, N. Kirichenko, and M. Kenis. **2019**. Safeguarding global plant health: the rise of sentinels. J. Pest Sci. (2004). 92: 29–36.

(FAOSTAT). **2021**. FAOSTAT.

Fried, G., B. Chauvel, P. Reynaud, and I. Sache. **2017**. Impact of Biological Invasions on Ecosystem Services. Impact Biol. Invasions Ecosyst. Serv.

Froissart, R., J. Doumayrou, F. Vuillaume, S. Alizon, and Y. Michalakis. **2010**. The virulence-transmission trade-off in vector-borne plant viruses: A review of (non-)existing studies. Philos. Trans. R. Soc. B Biol. Sci. 365: 1907–1918.

Frona, D., S. Janos, and M. Harangi-Rakos. **2019**. The Challenge of Feeding the World. MDPI J. Sustain. 3–4.

Hartman, G. L., J. C. Rupe, E. J. Sikora, L. L. Domier, J. A. Davis, and K. . Steffey. **2016**. Compendium of Soybean Diseases and Pests, Fifth Edition. Compend. Soybean Dis. Pests, Fifth Ed. 167–173.

Hashimi, M. H., R. Hashimi, and Q. Ryan. **2020**. Toxic Effects of Pesticides on Humans, Plants, Animals, Pollinators and Beneficial Organisms. Asian Plant Res. J. 5: 37–47.

Hayes, T. B., and M. Hansen. **2017**. From silent spring to silent night: Agrochemicals and the anthropocene. Elementa. 5.

Hershman, D. E., E. J. Sikora, and L. J. Giesler. **2011**. Soybean rust PIPE: Past, present, and future. J. Integr. Pest Manag. 2: 1–7.

Hofstra, N., and L. C. Vermeulen. **2016**. Impacts of population growth, urbanisation and sanitation changes on global human Cryptosporidium emissions to surface water. Int. J.

Hyg. Environ. Health. 219: 599–605.

Kalaitzandonakes, N., J. Kaufman, and K. Zahringer. **2019**. The Economics of Soybean Disease Contro. CABI.

Liebhold, A. M., and P. C. Tobin. **2006**. Growth of newly established alien populations: comparison of North American gypsy moth colonies with invasion theory. Popul. Ecol. 48: 253–262.

Mehrabi, Z., E. C. Ellis, and N. Ramankutty. **2018**. The challenge of feeding the world while conserving half the planet. Nat. Sustain. 1: 409–412.

Miller, S. A., F. D. Beed, and C. L. Harmon. **2009**. Plant disease diagnostic capabilities and networks. Annu. Rev. Phytopathol. 47: 15–38.

Nicolopoulou-Stamati, P., S. Maipas, C. Kotampasi, P. Stamatis, and L. Hens. **2016**. Chemical Pesticides and Human Health: The Urgent Need for a New Concept in Agriculture. Front. Public Heal. 4: 1–8.

Pagan, I., and F. Garcia-Arenal. **2020**. Tolerance of Plants to Pathogens: A Unifying View. Annu. Rev. Phytopathol. 58: 77–96.

Pan, Z., X. B. Yang, S. Pivonia, L. Xue, R. Pasken, and J. Roads. **2006**. Long-term prediction of soybean rust entry into the continental United States. Plant Dis. 90: 840–846.

Poland, T. M., and D. G. Mccullough. **2005**. Emerald Ash Borer: Invasion of the Urban Forest and the threat to North America's ash resource. J. For. 1990: 118–124.

Sacristán, S., and F. García-Arenal. **2008**. The evolution of virulence and pathogenicity in plant pathogen populations. Mol. Plant Pathol. 9: 369–384.

Sagar, A., and J. Dheeba. **2020**. On using transfer learning for plant disease detection. bioRxiv.

Sahu, S. K., M. Pandey, and K. Geete. **2021**. Classification of Soybean Leaf Disease from

Environment effect Using Fine Tuning Transfer Learning. 25: 2188–2201.

Savary, S., L. Willocquet, S. J. Pethybridge, P. Esker, N. McRoberts, and A. Nelson. **2019**. The global burden of pathogens and pests on major food crops. Nat. Ecol. Evol. 3: 430–439.

Sharma, A., V. Kumar, B. Shahzad, M. Tanveer, G. P. S. Sidhu, N. Handa, S. K. Kohli, P. Yadav, A. S. Bali, R. D. Parihar, O. I. Dar, K. Singh, S. Jasrotia, P. Bakshi, M. Ramakrishnan, S. Kumar, R. Bhardwaj, and A. K. Thukral. **2019**. Worldwide pesticide usage and its impacts on ecosystem. SN Appl. Sci. 1: 1–16.

Sharma, A., A. Shukla, K. Attri, M. Kumar, P. Kumar, A. Suttee, G. Singh, R. P. Barnwal, and N. Singla. **2020**. Global trends in pesticides: A looming threat and viable alternatives. Ecotoxicol. Environ. Saf. 201: 110812.

Sikora, E. J., T. W. Allen, K. A. Wise, G. Bergstrom, C. A. Bradley, J. Bond, D. Brown-Rytlewski, M. Chilvers, J. Damicone, E. DeWolf, A. Dorrance, N. Dufault, P. Esker, T. R. Faske, L. Giesler, N. Goldberg, J. Golod, I. R. G. Gómez, C. Grau, A. Grybauskas, G. Franc, R. Hammerschmidt, G. L. Hartman, R. A. Henn, D. Hershman, C. Hollier, T. Isakeit, S. Isard, B. Jacobsen, D. Jardine, R. Kemerait, S. Koenning, M. Langham, D. Malvick, S. Markell, J. J. Marois, S. Monfort, D. Mueller, J. Mueller, R. Mulrooney, M. Newman, L. Osborne, G. B. Padgett, B. E. Ruden, J. Rupe, R. Schneider, H. Schwartz, G. Shaner, S. Singh, E. Stromberg, L. Sweets, A. Tenuta, S. Vaiciunas, X. B. Yang, H. Young-Kelly, and J. Zidek. **2014**. A coordinated effort to manage soybean rust in North America: A success story in soybean disease monitoring. Plant Dis. 98: 864–875.

Tudi, M., H. D. Ruan, L. Wang, J. Lyu, R. Sadler, D. Connell, C. Chu, and D. T. Phung. **2021**. Agriculture development, pesticide application and its impact on the environment.

Int. J. Environ. Res. Public Health. 18: 1–24.

Zadoks, J. C., and R. D. Schein. **1979**. Epidemiology and Plant Disease Management. Epidemiol. Plant Dis. Manag. 427.

Chapter II: Soybean Disease Identification Using Original Field Images and Transfer Learning with Convolutional Neural Networks

Noah Bevers[1], Edward J. Sikora[1], and Nate B Hardy[1]

[1]*Department of Entomology and Plant Pathology, Auburn University*

301 Funchess Hall Auburn University, AL, USA 36849-5413

Noah Bevers, nzb0054@auburn.edu

Edward J. Sikora, sikorej@auburn.edu

Nate B Hardy, nbh0006@auburn.edu

Abstract

Meeting the growing demand for soybeans will require increased production. One approach would be to reduce yield loss from plant diseases. In the U.S., soybean diseases account for approximately 8-25% of average annual yield loss. Early and accurate detection of pathogens is key for effective disease management strategies and can help to minimize pesticide usage and thus boost overall productivity. Recent advancements in computer vision could move us towards that goal by making disease diagnostics expertise more readily accessible to everyone. To that end, we developed an automated classifier of digital images of soybean diseases, based on convolutional neural networks (CNN). For model training and validation, we acquired more than 9,500 original soybean images, representing eight distinct disease and deficiency classes: (1) healthy/asymptomatic, (2) bacterial blight, (3) Cercospora leaf blight, (4) downy mildew, (5) frogeye leaf spot, (6) soybean rust, (7) target spot, and (8) potassium deficiency. To make

training more efficient we experimented with a variety of approaches to transfer learning, data engineering, and data augmentation. Our best performing model was based on the DenseNet201 architecture. After training from scratch, it achieved an overall testing accuracy of 96.8%. Experimenting with full or partial freezing of core DenseNet201 model weights did not improve performance. Neither did a deliberate effort to increase the diversity of subject backgrounds in the digital images. On the other hand, data augmentation to increase representational parity across disease classes provided a substantial performance boost. Our development experience may provide useful insights for researchers considering the development of similar applications.

Keywords

Convolution, transfer learning, augmentation, soybean, disease diagnostics, image classification

Introduction

Over the last 60 years, soybean (*Glycine max* (L) Merrill) has become the world's premier oilseed crop and one of the five most important food crops worldwide (Savary et al. 2019). The land area devoted to soybean production has increased by 2.7% per year since 1964; a growth rate higher than that for any other major crop (Hartman et al. 2011, Kalaitzandonakes et al. 2019) Soybeans are usually processed into meal or oil (Ali 2010). The meal is high in protein and is used primarily as feed for livestock, in particular, poultry and swine; it is also commonly used in aquacultural production systems (Hartman et al. 2011). Soybean oil is mostly used for human consumption, but it is also used for a variety of industrial applications including the formulation of inks, paints, detergents, and lubricants (Kalaitzandonakes et al. 2019). Use in biodiesel production may also soon be significant (Kalaitzandonakes et al. 2019). But the most likely

increases in demand will come from the challenge of keeping growing human populations fed. Meeting these future demands for soybean will require creative solutions to current production limitations. Here, we focus on production losses caused by pathogens.

Plant pathogens cause hundreds of billions of dollars in crop losses per year (Fried et al. 2017). Soybean farms are no exception; in the United States (Hartman et al. 2016), and abroad (Oerke 2006, Wrather et al. 2010, Kalaitzandonakes et al. 2019), soybean diseases account for approximately 8-25% of the average annual yield loss (Hartman et al. 2016, Savary et al. 2019, Bradley et al. 2020). Across the USA, an estimated $45 USD per acre is lost annually due to the presence of 28 soybean diseases and pathogens; resulting in approximately $3.9 billion USD in annual yield losses (Bradley et al. 2020). Added to these direct costs are the costs of pesticide application and concomitant environmental degradation. Moreover, the liberal application of pesticides hastens the evolution of resistance in pest populations, and thus threatens the long-term sustainability of soybean farming. For example, in several regions of the USA, heavy reliance on quinone outside inhibitor (QoI) fungicides for the control of frogeye leaf spot disease in soybean has led to the development of several QoI fungicide-resistant isolates of the disease's causal agent, *Cercospora sojina* (Zeng et al. 2015). This has rendered QoI fungicides useless in some areas. The cost of developing a new pesticide for regulated usage can be up to $286 million USD (Kalaitzandonakes et al. 2019). Soybean farming would be more sustainable and better able to meet global food demands if soybean pesticide applications were more precise.

E**Error! Bookmark not defined.**arly and accurate detection of pathogens is crucial for applying effective management strategies and for developing coordinated disease and resistance

monitoring programs at local, regional, national, and global scales (Sikora et al. 2014). Early detection can also help to minimize pesticide usage which may ultimately slow the development of pesticide resistance. Many soybean diseases display progressive visual symptoms on the leaves of the plant such as discoloration, blotching, spotting, and lesion formation. Some of these diseases can be diagnosed by the trained eye of an experienced farmer, extension agent, or professional plant pathologist (Miller et al. 2009). But soybean producers may lack such expertise, and in some cases even an expert's eye is not enough. Thus, there is a need to improve the speed and accuracy of disease diagnostics. That need could be met with new technologies (Miller et al. 2009).

Recent advancements in deep learning and computer vision have the potential of democratizing disease diagnostics expertise and thereby increasing the precision and economy of pest control. In the last decade, a variety of computational modeling methods have been applied in attempts to automate disease diagnostics from digital images (Shrivastava and Hooda 2014, Garcia et al. 2015, Mohanty et al. 2016, Shrivastava and Singh 2017, Wu et al. 2019, Karlekar and Seal 2020, Sagar and Dheeba 2020, Sahu et al. 2021). At the core of the most successful advancements are convolutional neural networks (CNNs) (Lecun et al. 2015).

Artificial neural networks are meta-models composed of many computational nodes, each of which is (or is akin to) a logistic regression model. Nodes are arranged in layers, and each node in a layer is connected to all nodes in each adjacent layer. More specifically, each node receives output signals from nodes in the upstream layer, integrates those inputs in a way that depends on activation weights and bias values assigned by the model, and then outputs a signal to nodes in

the downstream layer. Such models can be trained to learn the rules – which can be complex and non-linear – for making certain predictions or classifications from data, using an algorithm known as backpropagation to optimize a set of activation weights for the connections between nodes in the network. All artificial neural networks have an input layer (which takes a data vector), an output layer (which gives predictions or classifications), and one or more hidden layers that map inputs to outputs (Lecun et al. 2015). CNNs are a type of artificial neural network in which there can be several distinct types of hidden layers, among which are special convolutional layers (Albawi et al. 2017). A convolutional layer applies a convolution to the outputs of the layer upstream, with convolution being the technical term for what is essentially a filter that accentuates certain data features and makes it easier for subsequent layers to extract their meaning. For example, a convolution might sharpen the vertical edges of a digital image, or increase the light-dark contrast across all image pixels (Lecun et al. 2015, Albawi et al. 2017). CNNs have been used for speech recognition, object segmentation, and visual object recognition and classification (Lecun et al. 2015). In summary, CNNs are a type of artificial neural network that are good at solving problems that involve 'seeing,' that is parsing and interpreting a grid of light intensity values (Kim 2017).

The diagnosis of many soybean diseases entails expert visual assessment of infected tissues. This appears to be a classification problem well suited for a CNN. Our goal was to develop such an application, that is, a CNN-based automated classifier of digital images of soybean diseases.

Materials and Methods

Set Up

Previous work on building an automated soybean disease image classifier has been based on publicly available image databases which are of limited scope (disease classes) and depth (images per disease class), with only a few hundred images available for model training across all disease categories (Shrivastava and Hooda 2014, Garcia et al. 2015, Karlekar and Seal 2020). Furthermore, many of these images are dated, of low quality, and rather uniform in terms of their background/environmental conditions. Generally, CNNs perform best when trained on large data sets with a variety of image conditions (Barbedo 2018). Hence, we sought to develop a better training data set of soybean diseases. Of course, training data acquisition can be slow-going and expensive, and the training of models on large data sets can take an inordinate amount of computational resources and energy (Strubell et al. 2020). For these reasons, a key area in CNN research is figuring out how to train models more efficiently. So, in addition to building a better training data set, we experimented with several approaches for making the training process more efficient.

Over the course of two seasons of soybean production, we collected over 9,500 original field images of soybean leaves in eight distinct disease categories. These were (1) healthy-looking plants, and those displaying the symptoms of (2) bacterial blight, (3) cercospora leaf blight, (4) downey mildew, (5) frogeye leaf spot, (6) soybean rust, (7) target spot, and (8) potassium deficiency. We explored the effects of varying image backgrounds, and we also experimented with data augmentation techniques. After training data sets were assembled, we explored the effects of varying model architectural parameters, and in particular we leveraged transfer learning methods (Shin et al. 2016). With transfer learning, models that have been trained on large data sets to solve one type of classification problem are adapted to a related type of

classification problem (Tan et al. 2018). Such transferred models can apply the higher-level, more abstract lessons they have learned about seeing something in general to the problem of telling a few specific things apart. The upshot is that they work well when training data sets are relatively small. For the general problem of digital image classification, several high-performing models are available (Krizhevsky et al. 2012, Shin et al. 2016), all of which have been trained on the ImageNet dataset, which contains over fourteen million well-annotated images, representing over twenty thousand image classes (Fei-Fei et al. 2010, Krizhevsky et al. 2012). We explored the application of several of these high-performing image classifier models, namely, VGG16 (Simonyan and Zisserman 2015), ResNet50 (He et al. 2016), Xception (Chollet 2017), and DenseNet201 (Huang et al. 2017).

Data Collection

Soybean leaves were photographed during the 2020 and 2021 Alabama (southeastern USA) growing seasons in the months of August, September, and October. Examples of images can be seen in **Figure 2.1**. During the 2020 season, all photographs were captured using a Canon EOS 7D Mark II Digital SLR Camera (made in Japan) at the EV Smith Agricultural Research Station in Tallassee, Alabama, USA. The primary method was to walk through rows of planted soybean fields and capture images of a single soybean leaf showing symptoms of a known disease with the leaf still attached to the plant. The leaves photographed were 'taken opportunistically' in a known diseased area. We attempted to photograph leaves at various heights in the canopy in proportion to how disease symptoms were distributed. At the end of each such walk, 10-20 leaves of each different represented disease category were detached from the plant and then

immediately photographed while laid flat on the ground in trimmed grass or on a white surface (car hood).

The diseases photographed were limited to those that naturally occurred in the field. During 2020, we captured 4,181 images across five disease categories, namely, healthy (asymptomatic) plants, bacterial blight, Cercospora leaf blight, frogeye leaf spot, and soybean rust.

During the 2021 season, we captured 5,413 original images. To the five disease categories represented in the 2020 data set, we added two new diseases – downy mildew and target spot – along with a nutrient deficiency, namely potassium. All images of the potassium deficiency were taken at Cullars Rotation in Auburn, AL (Patterson et al. 2019). Images of target spot were from Brewton Agricultural Research Unit in Brewton, AL. All other disease categories were from the EV Smith Research station. We used a slightly modified version of the data acquisition process we had used the year prior. For about 70% of cases, the same Digital SLR camera was used, but for the other 30% we used a Motorola Moto Z2 Play smartphone (Motorola, Inc. in Chicago, Illinois). This was done to better approximate the types of images that might be taken by users of the application in the field, and to add variety to the dataset which might help the CNN distinguish between signal and noise. Another modification was to increase the proportion of images of detached leaves on varying backgrounds. Approximately 30% of images were of a single detached leaf in 2021. About half of the detached leaves were photographed with the leaf laid flat on the ground in trimmed grass and the other half laid flat on a white table. We also deliberately varied light conditions, with a close to even mix of subjects in full sun and in shade.

Across both seasons we amassed a total of 9,594 original images collected across eight disease/deficiency categories. To these original images, we added an average of 80 images per disease category from extension resources and the publicly available "Image Database of Plant Disease Symptoms (PDDB)" (Barbedo et al. 2016). See **Table 2.1** for count details and **Figure 2.1** for sample images.

Data Preprocessing and Augmentation

The dataset of images used for the training and testing of CNN models included 10,722 total images. A Python script was used to randomly apportion the data into a training set and a testing set. Specifically, ~85% (9,113) of the images were used to train models, and ~15% (1609) were used to test them. The testing set was further subdivided in a validation set of 533 images (33% of the testing set), used to compare the performance of different model architectures, and an assessment set of 1076 images (66% of the testing set) used to assess the accuracy of the optimized model. These ratios are fairly standard, and tend to strike a balance between model over-fitting and under-fitting (Karlekar and Seal 2020).

CNN models tend to learn best when each classification category has roughly the same number of images (Li et al. 2018). Image augmentation is a common practice used to artificially increase the number of images in a data set by applying various transformation to original images, such as rotating, zooming, reflecting, adjusting brightness, and adding noise. In addition to increasing parity across classes, data augmentation can also be used to simply increase the overall volume of training data.

In our data set, bacterial blight was represented by roughly half as many images as the other categories. To increase parity, we augmented the bacterial blight set by horizontally reflecting each original image. On top of that, image augmentation was performed across the training data set during all model training using the Keras ImagaDataGenerator class (Chollet 2015). This library class acts as a template of sorts and allows the models to use a new transformation of each original image during each epoch of the training process. After some initial experimentation, all CNN models were trained using ImagaDataGenerator settings that allowed for width and height shifts [0.2] (fraction of total width/height), brightness adjustment [0.9,1.1] (range for picking a shift value from), rotation [30] (degree range for random rotations), and vertical and horizontal reflection. Another image pre-processing step was to standardize image size. This size was 224 x 224 x 3 (RGB) for all models except for Xception, which used 299 x 299 x 3. Image normalization was performed to make sure that there was uniform data distribution in the range of [0,1] (Gianchandani et al. 2020). This was done automatically within ImageDataGenerator by rescaling image pixel values by the number of channels, i.e., 1/255 (Chollet 2015).

Other possible pre-processing techniques such as object segmentation or grayscaling were not implemented, following previous work (Mohanty et al. 2016, Ferentinos 2018) demonstrating that they do not tend to improve final model performance for foliar disease diagnostics.

Model Design

Training

T**Error! Bookmark not defined.**raining a CNN is a special case of supervised machine learning. We provide the model with labeled training data – here, a set of classified images – and the model learns rules for classification that it can then apply to unlabeled data. In CNNs, this learning process is made more efficient by some elements of the model architecture. Concretely, feature extraction is performed via convolutional layers, feature reduction is then performed by pooling layers, and then classification is done with a softmax layer (Wang et al. 2018, Chen et al. 2020).

Training and testing of the models was implemented using Tensorflow (Abadi et al. 2016) and Keras (Chollet 2015) in a Linux environment on a shared computer cluster using an NVIDIA T4 Tensor Core GPU. Following the transfer-learning approach, baseline CNN architectures with weights pre-trained on the ImageNet dataset (Fei-Fei et al. 2010) were slightly altered with additional layers and then re-trained on our soybean image dataset. We compared the performance of several general-purpose CNN architectures while varying model parameters and data augmentation techniques.

Model Comparisons and Parameters -Base Models from Scratch

There are two main approaches to transfer learning. In the first, which we refer to as the 'frozen-core' approach, the pre-trained, core fully-connected model weights are fixed, and only the newly appended fully-connected layers of the network are trained on a new data set. In the second, known as 'training from scratch' the pre-trained layer weights are not fixed, but rather are used as a starting point, and all model weights are updated while training on new data. In other words, the entire model is trained. A previous study investigating CNN model performance

trained with over 900 ferrograph images found that DenseNet and ResNet base model architectures had higher accuracy when 'trained from scratch' (Peng and Wang 2020). We began with that approach.

The general template for the CNN architectures we implemented is shown in Figure 2.2. The base models (VGG16, ResNet50, Xception, and DenseNet201) initiated with pre-trained ImageNet weights and their respective layers were used for feature extraction. The last, fully-connected layer of each model was dropped. In its place we added architectural elements following the work of Gianchandani 2020 (Gianchandani et al. 2020). This comprised four new layers: (1) a global average pooling layer to reduce the number of parameters, (2) a fully connected layer of 128 neurons with a relu activation function and dropout of 0.2, (3) another fully connected layer of 64 neurons with relu activation and a dropout of 0.3, and (4) a fully-connected layer with softmax activation for eight-class classification of the different soybean disease categories. To reiterate, while training such models from scratch, none of the core layers are frozen; the pre-trained ImageNet weights are starting points for whole-network training.

After experimenting with various hyperparameter values to optimize accuracy on partial datasets, we standardized them across model experiments in order to allow for fair comparison. The hyperparameters used across all base models were: Learning rate: 0.0001, Optimizer = Stochastic Gradient Descent, Momentum = 0.9, Loss = Categorical Cross-Entropy, Batch size = 32, Epochs = 100. Additionally, upon literature review, we decided to use stochastic gradient descent as our optimization method because it has been shown to have higher generalization performance as compared to other adaptative optimization methods (Keskar and Socher 2017).

Alternative Fine-Tuning Strategies

After comparing the performance of the different base model architectures trained from scratch, we decided to further investigate the potential of transfer learning with other fine-tuning strategies. For this, we used the architecture which performed best when trained from scratch, namely, that with DenseNet201 as the base. First, we tried freezing the frozen-core approach. For this, we kept learning rate at 0.0001, but allowed for more training time, setting the number of training epochs to 150. With this approach, we sought to fully leverage the pre-trained ImageNet weights.

Next, we implemented a fine-tuning strategy with partial freezing. Initially, we again froze the core layers and only allowed the added fully-connected layers to update. For this stage, we increased the learning rate to 0.001 and trained for 90 epochs. Then, we unfroze all layers of the model, lowered the learning rate back to 0.0001, and trained for a further 10 epochs (for a total of 100 epochs). Thus, this approach can be seen as combination of the frozen-core and from-scratch approaches.

Model sensitivity to variation in training data

We also wanted to get a sense for how model performance was affected by variation in the training data. In particular, we were curious about the impact of adding the augmented (horizontally flipped) bacterial images on model performance, as well as the impact of the mix of subject backgrounds, that is, whether attached or severed leaves were photographed. For the

former, we removed the 484 additional bacterial blight augmented images from the training dataset and retrained from scratch the architecture using the DenseNet201 base model.

To quantify the effect of different subject backgrounds, we curated three different training datasets consisting of varying proportions of attached and severed leaf images. To reiterate, severed leaves were detached from the plant and photographed on either the ground in trimmed grass or on a white background of a (tabletop or car hood). The three datasets consisted of (100% attached/ 0% severed), (75% attached/ 25% severed), and (50% attached/ 50% severed).

In order to maximize the variety of proportions of attached and severed leaves that we could analyze, each of the image databases contained 4500 original images. As for the main analyses, a Python script was used to randomly apportion the data into a training set and a testing set with a 85:15 split. For these comparisons, as an expediency we used a ResNet50 base model trained from scratch implementing the same hyperparameters as previously described for scratch models. Models based on ResNet50 performed nearly as well as those based on DenseNet201 but were trained more efficiently.

Performance Metrics

Model performances were tested using 1076 previously unseen test images and were evaluated using quantitative metrics derived from a confusion matrix. These metrics include accuracy, precision, recall, and F-1 scores. Accuracy is often considered the model's overall performance and calculates the correctly predicted labels by the equation (Basavegowda and Dagnew 2020, Gianchandani et al. 2020):

Accuracy = $\frac{True\ Positives + True\ Negatives}{True\ Positives + True\ Negatives + False\ Positives + False\ Negatives}$

Precision is used to evaluate the exactness of the predictions by comparing the correctly predicted number of images in a disease category with the total number predicted in that category by the model (Gianchandani et al. 2020): Precision = $\frac{True\ Positives}{True\ Positives + False\ Positives}$

Recall uses a ratio for the number of correctly predicted images in a disease category compared to all actual observations of that category. A higher recall implies better ability to predict both positive and negative observations (Goutte and Gaussier 2005, Gianchandani et al. 2020): Recall = $\frac{True\ Positives}{True\ Positives + False\ Negatives}$

The F1-score is an integrative measure that combines precision and recall (Gianchandani et al. 2020): F1-Score = $\frac{2\ x\ Precision\ x\ Recall}{Precision + Recall}$

Loss and accuracy plots were generated using *ggplot2* (Wickham 2011) in R studio (R Core Team 2019).

Results

Model Performance Comparisons

The relative performances of transfer-learning architectures trained from scratch and based on VGG16, Xception, ResNet50, and DenseNet201, as well as the additional fine-tuning and augmentation models using DenseNet201 are summarized in **Table 2.2**. The highest overall

testing accuracy, 96.8%, was achieved with the base model architecture of DenseNet201 trained from scratch (**Figure 2.3**). This model was closely followed by the model based on ResNet50, and then next by the Xception and VGG16 architectures. The DenseNet201 from-scratch model also had the highest precision, recall, and F1-score metrics. The ResNet50 model was the fastest to train for the from-scratch models. The DenseNet201 models that implemented full or partial freezing of the core model weights both decreased the amount of total training time but diminished the overall model performance. The partial-freezing approach had the shortest total training time.

The training and validation loss for the from-scratch DenseNet201 model can be seen in **Figure 2.4** where both plots follow a similar trend with approximately similar values; training and validation are simultaneously and continuously maximizing accuracy while minimizing loss. This is desirable and it appears that any slight over-fitting that may be occurring between training and validation did not significantly impact the model's ability to make correct predictions and maintain high accuracy (96.8%) on unseen test data.

Figure 2.5 shows a confusion matrix for the DenseNet201 from-scratch model (Cipriano 2018). The model's worst precision was bacterial blight. It predicted bacterial blight as the disease 118 times when there were only 108 actual bacterial blight images. The model's worst recall was for soybean rust. The model correctly predicted 163 out of 175 soybean rust images (93.14%). The model had the best performance on potassium deficiency, which it correctly identified in all 109 cases.

Model sensitivity to variation in training data

Removing the additional augmented bacterial blight images had slightly negative effects on the overall model performance using the scratch DenseNet201 base model architecture (as seen in **Table 2.2**). The effect was more pronounced on the bacterial blight category specifically. Removal of the additional augmented images resulted in a precision decrease for bacterial blight images from 89.83% to 82.86% and a recall decrease from 98.15% to 96.67%. The model trained without the additional augmented images was not as good at being able to predict or recognize bacterial blight.

Comparisons of model performances depending on the mix of attached and severed leaf images are summarized in **Table 2.3**. As a reminder, these models used a ResNet50 base model architecture to save on computing time. The best performance was from the dataset that included only attached leaf field images (100% Attached / 0% Severed). In fact, the trend appears to be that overall model performance slightly decreased as more severed leaf images were included in the datasets.

Error! Bookmark not defined.

We have deployed our soybean foliar disease classifier to the web at http://sickbeans.skullisland.info. Codes used for model specification and training are available in a github repository (https://github.com/nzb0054/RoboCrop-CNN-WebApp).

Discussion

Our goal was to develop an application to make soybean disease identification more accessible and to assist with early and accurate detection of pathogens as part of an effective management

strategy. Our approach was to train a CNN, and to explore ways of making that training process more efficient. We focused on the application of transfer learning. Several high-performing, general-purpose computer vision networks are available for this purpose. We found that, for soybean foliar disease classification, the best performing base model was DenseNet201, using the from-scratch training approach. Using that model, we were able to develop an application that distinguishes between eight soybean disease/deficiency classes with an overall accuracy of 96.75%. Moreover, we could do so with a training data set that although significantly larger than what has been previously available, was still quite feasible to assemble. Hence, we find that the state of deep learning technology has advanced to the point where high-performance automated plant disease diagnostics is quite a reachable goal. With freely-available general-purpose computer vision models it would seem possible to develop custom computer vision applications with only about 1000 images of each class. Of course training data acquisition and model training still take substantial investments, but once the model is trained, its application is rather simple (Mohanty et al. 2016). We have deployed our model, which we call RoboCrop, to the web at http://sickbeans.skullisland.info.

With a smartphone, users can take a picture of a diseased soybean leaf in the field, upload the image to the web application, then the app will return a diagnosis almost instantly along with links to further extension resources for confirmation and management options. Pathogen identification is an important first step in determining if pesticide or fungicide application is necessary. In the southern USA, for example, spraying fungicides is often required for the treatment of soybean rust, frogeye leaf spot, and, occasionally, target spot. In comparison, spraying is not usually recommended or economical for bacterial blight, downey mildew, and

cercospora leaf blight. Being able to distinguish between these diseases can help to inform a farmer whether or not they should be considering fungicide applications. Hopefully, our application will assist with reducing excessive use of pesticides and thereby forestall the evolution of pesticide resistance.

Some caveats are in order. We sought to collect a comprehensive set of images, portraying the symptoms of soybean diseases that are common in our area, under a variety of field conditions. Nevertheless, given logistical constrains, our training data set still has strong spatial and temporal biases. We will get a better sense for the robustness of the model as it is deployed more broadly over space and time. That being said, because our web application retains user submission, we are optimistic that with iterative model training, the application will become more robust and comprehensive as it is more widely deployed (Shin et al. 2016).

While assembling our training data, we deliberately sought to acquire images of subjects in a variety of settings, that is, with different backgrounds. We put special emphasis on photographing a mix of attached and severed leaves. We expected that this would help the CNN learn to disregard spurious background information and hone in on subject features. Contra to this expectation, we found that models perform better when they are trained exclusively on images of attached leaves. Conversely, increasing the proportion of severed leaf images reduces model performance. It is possible that this is an artifact of reducing the total size of the training dataset so that we could manipulate the ratios of attached and severed leaf images. It is also possible that there is genuinely useful information in the background of an image about the health state of a subject, for example, the overall structure of the canopy or the contrast of leaf

colors. If the inferred positive effects of attached leaf images are reliable, this would make further data collection easier, and best practices for obtaining query images more convenient. It is less work to take a picture of an attached leaf.

Our development experience suggests that researchers planning to develop similar diagnostic applications should consider data augmentation as a way of increasing parity among classes. Our top-performing model has the most difficulty (in the sense of the lowest precision) recognizing bacterial blight. Simply put, the model often predicted bacterial blight as the disease category when that was not the case. CNNs typically perform best with large, balanced datasets (Li et al. 2018) and bacterial blight had the least representation of any category. We attempted to remedy this by doubling the bacterial blight images used in the original training set through data augmentation (horizontal flipping). This technique appears to have been effective. Omitting these additional, augmented images diminished overall model performance and caused a noticeable decline in the precision and recall scores for the bacterial blight disease category. Experimenting more deeply with the further addition of augmented original images for all disease categories might allow for further increases in model performance. In sum, it appears that training data limitations underlie some of the shortcomings in model performance, and hence additional data should continue to improve its performance.

Developers might also consider frozen-core approaches for the initial stages of model training and evaluation. In our experiments with these approaches, in comparison to from-scratch training, model performance was somewhat diminished, but the training time was considerably

reduced. Thus, frozen-core approaches could alleviate some of the computational cost of model training.

Conclusion

In conclusion, with mostly off-the-shelf neural network architectures, and with digital images of diseased soybean plants taken by a single researcher over the course of two seasons, we were able to develop an automated classifier of soybean foliar diseases that accurately predicted disease classes in more than 95% of the cases. Ideally, for the application to be developed further into a tool that farmers will find useful, a comprehensive collection of soybean diseases can be acquired as the seasons progress. The identification application should be further tested with various camera devices in a geographically diverse set of field environments to quantify more generalized performance. Application functionality and optimization of user interface ought to be updated based on the practical needs and suggestions of growers. Ideally, continuous iterations of model building and upgrading of the application will take place. There is certainly the opportunity for more user-related and field specific information to be integrated into the application. This could potentially push the application beyond just disease identification and lead to a more extensive management resource and decision-making tool for agricultural systems. The soybean disease classifier presented here is an optimistic step toward the goal of making high-performance automated plant disease diagnostics more accessible to all.

Acknowledgements

This work was supported by the Alabama Soybean Producers Association and the Alabama Agricultural Experiment Station (AAES).

References – Chapter II

Abadi, M., A. Agarwal, P. Barham, E. Brevdo, Z. Chen, C. Citro, G. S. Corrado, A. Davis, J. Dean, M. Devin, S. Ghemawat, I. Goodfellow, A. Harp, G. Irving, M. Isard, Y. Jia, R. Jozefowicz, L. Kaiser, M. Kudlur, J. Levenberg, D. Mane, R. Monga, S. Moore, D. Murray, C. Olah, M. Schuster, J. Shlens, B. Steiner, I. Sutskever, K. Talwar, P. Tucker, V. Vanhoucke, V. Vasudevan, F. Viegas, O. Vinyals, P. Warden, M. Wattenberg, M. Wicke, Y. Yu, and X. Zheng. **2016**. TensorFlow: Large-Scale Machine Learning on Heterogeneous Distributed Systems.

Albawi, S., T. A. M. Mohammed, and S. Alzawi. **2017**. Understanding of a Convolutional Neural Network. Ieee. 16.

Ali, N. 2010. The soybean: botany, production and uses. CABI.

Barbedo, J. G. A. 2018. Impact of dataset size and variety on the effectiveness of deep learning and transfer learning for plant disease classification. Comput. Electron. Agric. 153: 46–53.

Barbedo, J. G. A., L. V. Koenigkan, and T. T. Santos. **2016**. Identifying multiple plant diseases using digital image processing. Biosyst. Eng. 147: 104–116.

Basavegowda, H. S., and G. Dagnew. **2020**. Deep learning approach for microarray cancer data classification. CAAI Trans. Intell. Technol. 5: 22–33.

Bradley, C., T. W. Allen, A. J. Sisson, G. C. Bergstrom, K. M. Bissonnette, J. Bond, E. Byamukama, M. I. Chilvers, A. A. Collins, J. P. Damicone, A. E. Dorrance, N. S. Dufault, P. D. Esker, T. R. Faske, N. M. Fiorellino, L. J. Giesler, G. L. Hartman, C. A. Hollier, T. Isakeit, T. A. Jackson-Ziems, D. J. Jardine, H. M. Kelly, R. C. Kemerait, N.

M. Kleczewski, A. M. Koehler, R. J. Kratochvil, J. E. Kurle, D. K. Malvick, S. G. Markell, F. M. Mathew, H. L. Mehl, K. M. Mehl, D. S. Mueller, J. D. Mueller, B. D. Nelson, C. Overstreet, G. B. Padgett, P. P. Price, E. J. Sikora, I. Small, D. L. Smith, T. N. Spurlock, C. A. Tande, D. E. P. Telenko, A. U. Tenuta, L. D. Thiessen, F. Warner, W. J. Wiebold, and K. Wise. **2020**. Soybean yield loss estimates due to diseases in the United States and Ontario, Canada, from 2015 to 2019. Plant Heal. Prog. 21: 238–247.

Chen, J., J. Chen, D. Zhang, Y. Sun, and Y. A. Nanehkaran. **2020**. Using deep transfer learning for image-based plant disease identification. Comput. Electron. Agric. 173: 105393.

Chollet, F. 2015. Keras.

Chollet, F. 2017. Xception: Deep learning with depthwise separable convolutions. Proc. - 30th IEEE Conf. Comput. Vis. Pattern Recognition, CVPR 2017. 2017-Janua: 1800–1807.

Cipriano, W. 2018. Pretty Print Confusion Matrix.

(FAOSTAT) . **2021**. FAOSTAT.

Fei-Fei, L., J. Deng, and K. Li. **2010**. ImageNet: Constructing a large-scale image database. J. Vis. 9: 1037–1037.

Ferentinos, K. P. 2018. Deep learning models for plant disease detection and diagnosis. Comput. Electron. Agric.

Fried, G., B. Chauvel, P. Reynaud, and I. Sache. **2017**. Impact of Biological Invasions on Ecosystem Services. Impact Biol. Invasions Ecosyst. Serv.

Garcia, J., A. Barbedo, and C. V. Godoy. **2015**. Automatic Classification of Soybean Diseases Based on Digital Images of. X Sbi Agro.

Gianchandani, N., A. Jaiswal, D. Singh, V. Kumar, and M. Kaur. **2020**. Rapid COVID-19

diagnosis using ensemble deep transfer learning models from chest radiographic images. J. Ambient Intell. Humaniz. Comput.

Goutte, C., and E. Gaussier. **2005**. A Probabilistic Interpretation of Precision, Recall and F-Score, with Implication for Evaluation. Lect. Notes Comput. Sci. 3408: 345–359.

Hartman, G. L., J. C. Rupe, E. J. Sikora, L. L. Domier, J. A. Davis, and K. . Steffey. **2016**. Compendium of Soybean Diseases and Pests, Fifth Edition. Compend. Soybean Dis. Pests, Fifth Ed. 167–173.

Hartman, G. L., E. D. West, and T. K. Herman. **2011**. Crops that feed the World 2. Soybean-worldwide production, use, and constraints caused by pathogens and pests. Food Secur. 3: 5–17.

He, K., X. Zhang, S. Ren, and J. Sun. **2016**. Deep residual learning for image recognition. Proc. IEEE Comput. Soc. Conf. Comput. Vis. Pattern Recognit. 2016-Decem: 770–778.

Huang, G., Z. Liu, L. Van Der Maaten, and K. Q. Weinberger. **2017**. Densely connected convolutional networks. Proc. - 30th IEEE Conf. Comput. Vis. Pattern Recognition, CVPR 2017. 2017-Janua: 2261–2269.

Kalaitzandonakes, N., J. Kaufman, and K. Zahringer. **2019**. The Economics of Soybean Disease Contro. CABI.

Karlekar, A., and A. Seal. **2020**. SoyNet: Soybean leaf diseases classification. Comput. Electron. Agric. 172.

Keskar, N. S., and R. Socher. **2017**. Improving Generalization Performance by Switching from Adam to SGD.

Kim, P. 2017. Convolutional Neural Network. MATLAB Deep Learn. 121–147.

Krizhevsky, B. A., I. Sutskever, and G. E. Hinton. **2012**. ImageNet Classification with Deep

Convolutional Neural Networks. Commun. ACM. 60: 84–90.

Lecun, Y., Y. Bengio, and G. Hinton. **2015**. Deep learning. Nature. 521: 436–444.

Li, S., W. Song, H. Qin, and A. Hao. **2018**. Deep variance network: An iterative, improved CNN framework for unbalanced training datasets. Pattern Recognit. 81: 294–308.

Miller, S. A., F. D. Beed, and C. L. Harmon. **2009**. Plant disease diagnostic capabilities and networks. Annu. Rev. Phytopathol. 47: 15–38.

Mohanty, S. P., D. P. Hughes, and M. Salathé. **2016**. Using deep learning for image-based plant disease detection. Front. Plant Sci. 7: 1–10.

Oerke, E. C. 2006. Crop losses to pests. J. Agric. Sci. 144: 31–43.

Patterson, P., D. Monks, C. Chen, and B. Ortiz. **2019**. Auburn University Crops. Cotton Report. 42: 49-51.

Peng, P., and J. Wang. **2020**. How to fine-tune deep neural networks in few-shot learning?

R Core Team, R. F. for S. C. 2019. R: A Language and Environment.

Sagar, A., and J. Dheeba. **2020**. On using transfer learning for plant disease detection. bioRxiv.

Sahu, S. K., M. Pandey, and K. Geete. **2021**. Classification of Soybean Leaf Disease from Environment effect Using Fine Tuning Transfer Learning. 25: 2188–2201.

Savary, S., L. Willocquet, S. J. Pethybridge, P. Esker, N. McRoberts, and A. Nelson. **2019a**. The global burden of pathogens and pests on major food crops. Nat. Ecol. Evol. 3: 430–439.

Shin, H. C., H. R. Roth, M. Gao, L. Lu, Z. Xu, I. Nogues, J. Yao, D. Mollura, and R. M. Summers. **2016**. Deep Convolutional Neural Networks for Computer-Aided Detection: CNN Architectures, Dataset Characteristics and Transfer Learning. IEEE Trans. Med. Imaging. 35: 1285–1298.

Shrivastava, S., and D. S. Hooda. **2014**. Automatic Brown Spot and Frog Eye Detection from

the Image Captured in the Field. 4: 131–134.

Shrivastava, S., and S. K. Singh. **2017**. Soybean plant foliar disease detection using image retrieval approaches. 26647–26674.

Sikora, E. J., T. W. Allen, K. A. Wise, G. Bergstrom, C. A. Bradley, J. Bond, D. Brown-Rytlewski, M. Chilvers, J. Damicone, E. DeWolf, A. Dorrance, N. Dufault, P. Esker, T. R. Faske, L. Giesler, N. Goldberg, J. Golod, I. R. G. Gómez, C. Grau, A. Grybauskas, G. Franc, R. Hammerschmidt, G. L. Hartman, R. A. Henn, D. Hershman, C. Hollier, T. Isakeit, S. Isard, B. Jacobsen, D. Jardine, R. Kemerait, S. Koenning, M. Langham, D. Malvick, S. Markell, J. J. Marois, S. Monfort, D. Mueller, J. Mueller, R. Mulrooney, M. Newman, L. Osborne, G. B. Padgett, B. E. Ruden, J. Rupe, R. Schneider, H. Schwartz, G. Shaner, S. Singh, E. Stromberg, L. Sweets, A. Tenuta, S. Vaiciunas, X. B. Yang, H. Young-Kelly, and J. Zidek. **2014**. A coordinated effort to manage soybean rust in North America: A success story in soybean disease monitoring. Plant Dis. 98: 864–875.

Simonyan, K., and A. Zisserman. **2015**. Very deep convolutional networks for large-scale image recognition. 3rd Int. Conf. Learn. Represent. ICLR 2015 - Conf. Track Proc. 1–14.

Strubell, E., A. Ganesh, and A. McCallum. **2020**. Energy and policy considerations for modern deep learning research. AAAI 2020 - 34th AAAI Conf. Artif. Intell. 1393–13696.

Tan, C., F. Sun, T. Kong, W. Zhang, C. Yang, and C. Liu. **2018**. A Survey on Deep Transfer Learning. Int. Conf. Artif. neural networks. 1–10.

Wang, S. H., P. Phillips, Y. Sui, B. Liu, M. Yang, and H. Cheng. **2018**. Classification of Alzheimer's Disease Based on Eight-Layer Convolutional Neural Network with Leaky Rectified Linear Unit and Max Pooling. J. Med. Syst. 42: 1–11.

Wickham, H. 2011. Ggplot2. Wiley Interdiscip. Rev. Comput. Stat. 3: 180–185.

Wrather, A., G. Shannon, R. Balardin, L. Carregal, R. Escobar, G. K. Gupta, Z. Ma, W. Morel, D. Ploper, and A. Tenuta. **2010**. Effect of Diseases on Soybean Yield in the Top Eight Producing Countries in 2006. Plant Heal. Prog. 11: 29.

Wu, Q., K. Zhang, and J. Meng. **2019**. Identification of Soybean Leaf Diseases via Deep Learning. J. Inst. Eng. Ser. A. 100: 659–666.

Zeng, F., E. Arnao, G. Zhang, G. Olaya, J. Wullschleger, H. Sierotzki, R. Ming, B. H. Bluhm, J. P. Bond, A. M. Fakhoury, and C. A. Bradley. **2015**. Characterization of quinone outside inhibitor fungicide resistance in Cercospora sojina and development of diagnostic tools for its identification. Plant Dis. 99: 544–550.

Figures and Tables – Chapter II

Disease Category	2020 Original Images	2021 Original Images	Total Original Images	Additional Augmented Images	Extension Images	Images Used in Models
Bacterial Blight	484	0	484	484	104	1072
Cercospora Leaf Blight	1163	435	1598	0	38	1636
Downey Mildew	0	652	652	0	104	756
Frogeye Leaf Spot	495	1045	1540	0	110	1650
Healthy (Asymptomatic)	908	724	1632	0	31	1663
Potassium Deficiency	0	1034	1034	0	49	1083
Soybean Rust	1131	496	1627	0	127	1754
Target Spot	0	1081	1081	0	27	1108
Total	4181	5467	9648	484	590	10722

Table 2.1: Image Collection. Displays the total number of images for each disease category that were photographed for each season. Bacterial blight was the only category that used the addition of augmented images prior to model training. Image augmentation applies various transformations to original images, such as rotating, zooming, reflecting, adjusting brightness, and adding noise. Total images used across both training and testing can be seen in the far-right column.

Base Model Architecture	Accuracy	Precision	Recall	F1	Secs/Step	Secs/Epoch	Total Secs
VGG16 (Scratch)	**90.8**	**91.0**	**90.9**	**90.4**	**34.5**	**9868**	**986800**
Xception (Scratch)	**92.4**	**93.0**	**91.9**	**92.4**	**37.1**	**10621**	**1062100**
ResNet50 (Scratch)	**95.9**	**95.9**	**96.4**	**96.1**	**20.0**	**5783**	**578300**
DenseNet201 (Scratch)	**96.8**	**96.6**	**97.1**	**96.8**	**29.3**	**8398**	**839800**

DenseNet (No Extra Augmentation)	**96.7**	**95.9**	**97.1**	**96.4**	**29.0**	**7974**	**797400**
DenseNet (Fine-Tune 90/10 Epochs)	**94.9**	**95.5**	**94.9**	**95.1**	**12.8**	**3718**	**371800**
DenseNet (Freeze 150 Epochs)	**84.6**	**85.2**	**86.0**	**85.4**	**11.1**	**3270**	**490500**

Table 2.2: Model Performance Comparison. Test evaluation of each of base model architectures implemented.

Images Used in Dataset (ResNet50 Models)	**Accuracy**	**Precision**	**Recall**	**F1**
50% Attached / 50% Severed	**95.18**	**95.51**	**95.93**	**95.60**
75% Attached / 25% Severed	**96.48**	**96.54**	**96.53**	**96.50**
100% Attached / 0% Severed	**97.58**	**97.66**	**97.75**	**97.69**

Table 2.3: Model Performance of Differing Proportion of Attached and Severed Images. All models implemented an identical base model ResNet50 architecture from scratch with 4500 image datasets.

Figure 2.1: **Sample Images**. Examples of the photographed soybean leaves for all eight disease categories. Starting from left to right, top to bottom: bacterial blight, Cercospora leaf blight, downy mildew, frogeye, healthy/asymptomatic, potassium deficiency, soybean rust, target spot. Note some cropping was used here for display purposes.

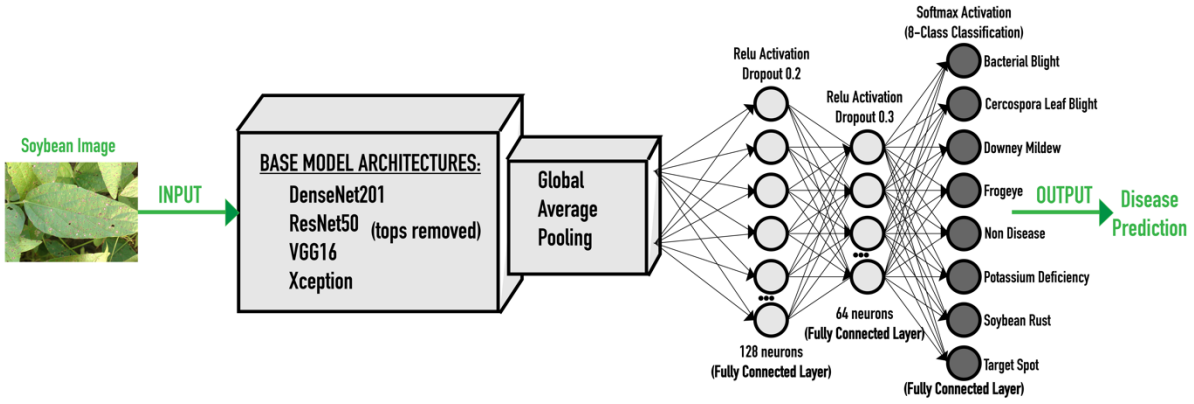

Figure 2.2: Convolutional Neural Network Model Architecture. A simplified graphic/template for all model architectures and standardized parameters. Within the base model 'box' is, in reality, each respective base model's full architecture without the last layer. All

models are initiated with the pre-trained ImageNet weights. For the 'scratch' models, all layer weights, including those inside the base model box are allowed to update (i.e., they are not frozen). For the additional DenseNet201 transfer learning models, the layers inside the box are frozen for a certain number of epochs.

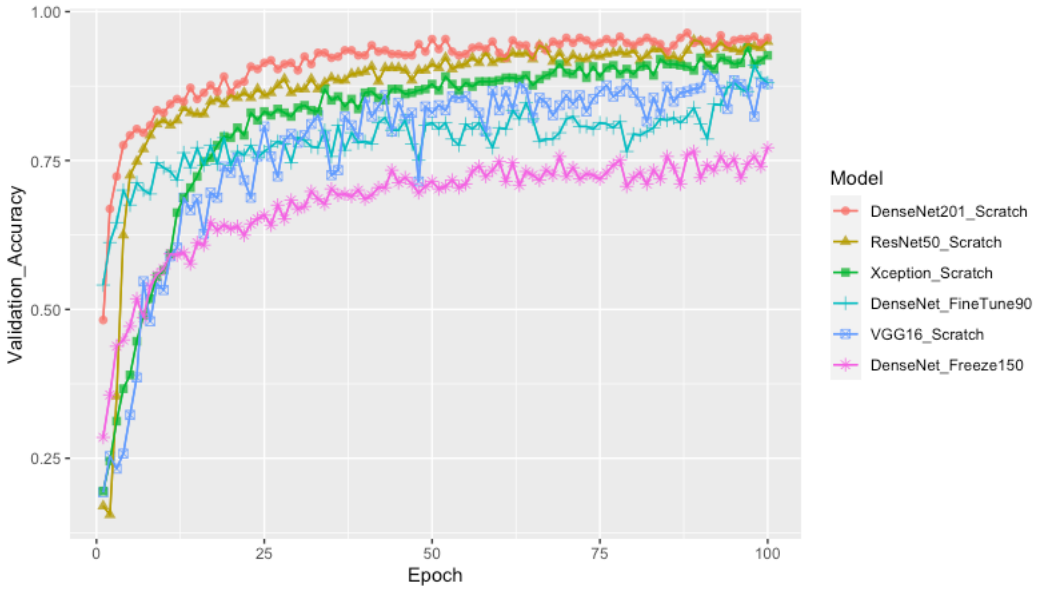

Figure 2.3: Accuracy Comparison. Accuracy of each model while trained through 100 epochs. Note that DenseNet_Freeze150 was trained for an additional 50 epochs not seen here, but it still maintained the lowest accuracy.

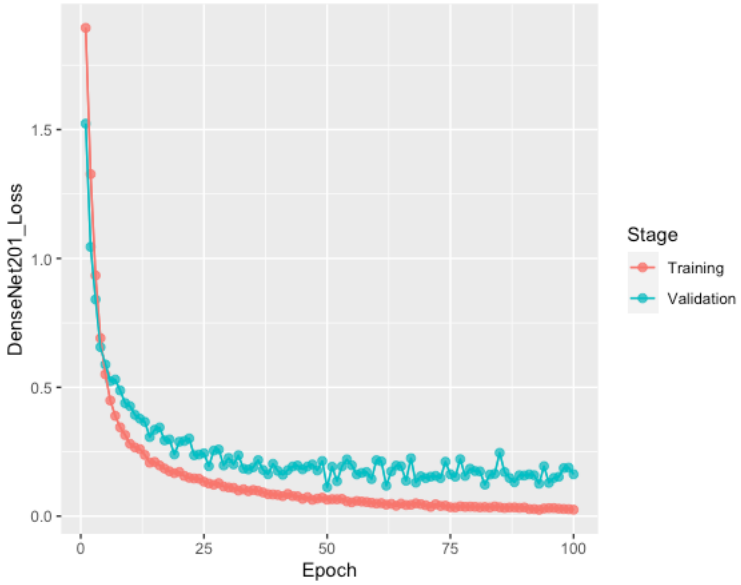

Figure 2.4: DenseNet201 Training Loss vs Validation Loss. Minimization of the loss function through 100 epochs for the training dataset compared to the validation dataset for DenseNet201.

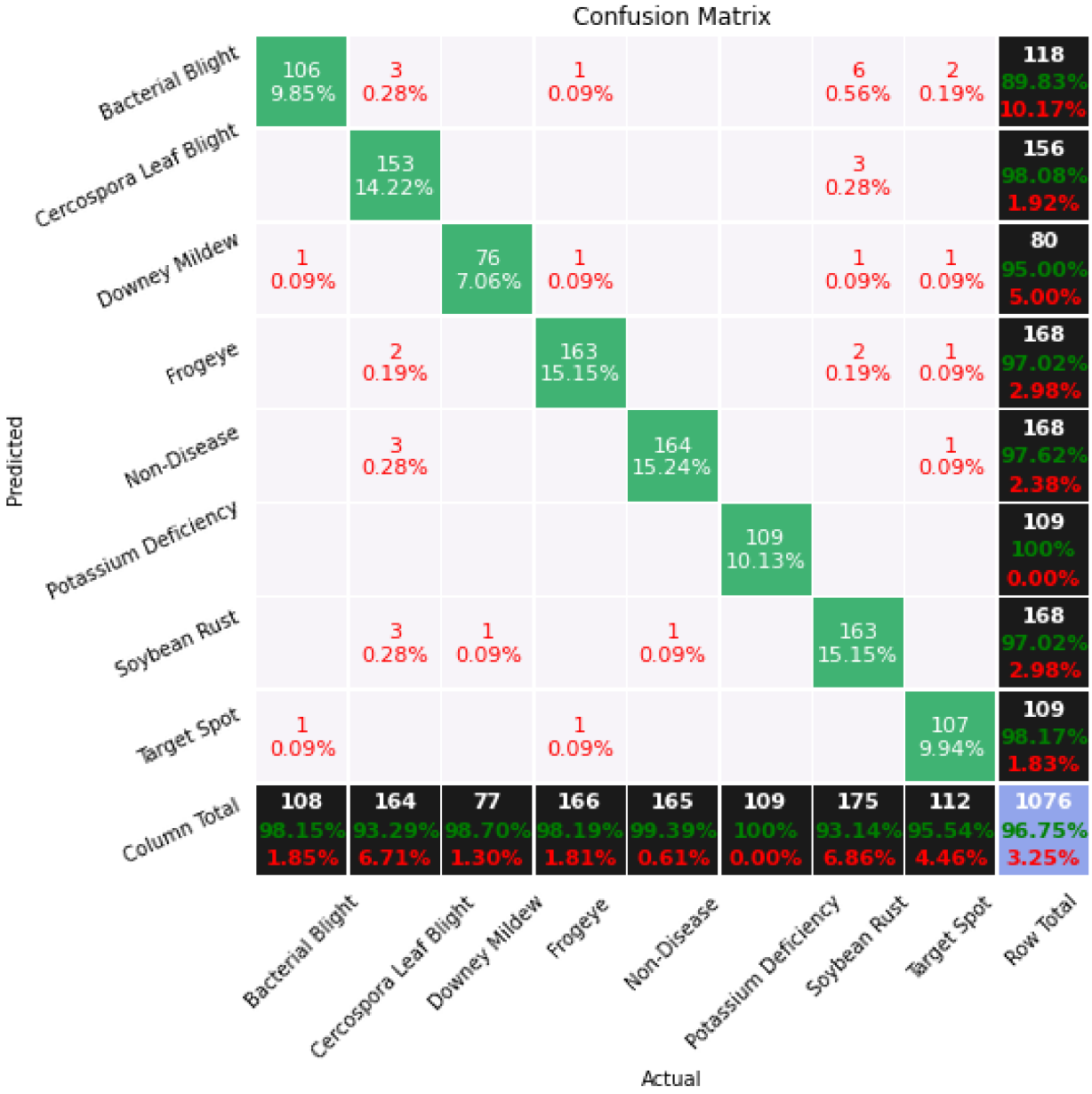

Figure 2.5: Confusion Matrix for DenseNet201 Base Model. The performance of trained models was tested using 1076 previously unseen test images. Model predicted categories for each test image can be read on the row values of the left (y-axis) as compared to the actual disease categories on the column values of the bottom (x-axis). The green diagonal boxes are filled with the correct number of predictions for that category. White boxes filled with red numbers are the number of incorrect predictions. The green numbers in the black boxes display

the precision and recall scores for each disease category. Precision scores are the green numbers within the black far-right column. Recall scores are within the black bottom right row. Overall model performance is in the blue bottom right box. 1041 correct predictions out of 1076 total test images; 96.75% accuracy.

Chapter III: Virulence is Correlated with Pathogen Accumulation in Plants

Noah Bevers, Gwendolyn Bird, Leonardo De La Fuente and Nate B Hardy
Department of Entomology and Plant Pathology, Auburn University

Noah Bevers, nzb0054@auburn.edu
Gwendolyn Bird, gmb0032@auburn.edu
Leonardo De La Fuente, lzd0005@auburn.edu
Nate B Hardy, nbh0006@auburn.edu

Abstract

Although simple epidemiological theory predicts that selection should be against it, pathogen populations often evolve high levels of virulence. According to the Trade-off Hypothesis this is because of pleiotropy; virulence is the byproduct of aggressive pathogen replication which increases instantaneous transmission rates. This hypothesis permeates theoretical work on virulence evolution and has broad empirical support from animal pathosystems. But the evidence from plants is conflicting. Moreover, two common features of plant pathosystems could break down a direct causal relationship between pathogen accumulation and virulence, to wit, immunopathology, and the preponderance of host genotypes that are tolerant to infection. To get a clearer view of the relationship between pathogen accumulation and virulence in plant pathosystems, we conducted a meta-analysis of 282 effect sizes from 18 empirical studies. We found that the overall relationship was positive and significant. We also found that the relationship varied widely across studies, and most of that variation could not be explained by the moderators in our model. Thus, the Trade-off Hypothesis predicts levels of virulence in plant pathosystems, but there are limits to its predictive power, and a deeper understanding virulence

evolution requires a more nuanced view of infection physiology, ecology, and population genetics.

Introduction

Pathogen strains vary in virulence, that is, the extent to which they harm their host (D'arcy et al. 2001, Sacristán and García-Arenal 2008). The Trade-off Hypothesis posits that virulence is the byproduct of aggressive pathogen replication (Anderson and May 1982, Bull and Lauring 2014). High within-host pathogen abundance increases the instantaneous rate of transmission between hosts. But it also increases host mortality and thereby decreases the overall time in which any one host can infect another. A variant of the Trade-off Hypothesis also allows for trade-offs involving the rate at which hosts recover from infection, but this complicates the analysis of virulence evolution, and in practice, theorists tend to fix recovery rates and focus on pathogen transmission rates and excess host-mortality (Cressler et al. 2016). With this constrain, the Trade-off Hypothesis predicts that every pathosystem has a level of virulence that optimizes overall pathogen transmission.

The Trade-off Hypothesis hinges on two fundamental assumptions about pathogen ecology: (i) virulence increases with within-host pathogen accumulation, and (ii) so do the odds of transmission for each contact between hosts, or between hosts and vectors (Bull 1994, Frank 1996, Froissart et al. 2010). For animal pathosystems, it would seem that these assumptions hold; a recent meta-analysis (Acevedo et al. 2019) recovered significant positive relationships between within-host pathogen accumulation and virulence, and between pathogen accumulation and transmission rate. But the validity of these assumptions for plant pathosystems is uncertain.

Researchers have consistently found a positive relationship between pathogen accumulation and transmission rate (Froissart et al. 2010), but the evidence is conflicting for how accumulation maps to virulence (eg, (Ebert and Mangin 1997, Lipsitch and Moxon 1997, Mackinnon and Read 2004, Jensen et al. 2006, Sacristán and García-Arenal 2008)).

In fact, two common features of plant pathosystems could break-down a direct causal relationship between pathogen accumulation and virulence. The first is tolerance; relative to susceptible host genotypes, tolerant genotypes are harmed less by a given pathogen load (Råberg 2014). Variation in tolerance among hosts can muddle the host-population-level link between pathogen accumulation and virulence (Miller et al. 2006, Pagan and Garcia-Arenal 2020). The second is immunopathology; much of the harm induced by plant pathogens is not through direct exploitation of host resources, but rather through the induction of self-harming immune responses, for example hypersensitive responses (Graham et al. 2005). Such immunopathological effects can depend little on pathogen load. To be clear, animal pathosystems can also entail tolerance and immunopathology; indeed, in animal-virus systems, viral replication often depends on inhibition of apoptosis (Lam et al. 2001). But since plants lack mobile and adaptive immune factors, the scope for tolerance variation and immunopathology might be greater.

The evolution of virulence in plant pathogens has enormous economic and social impacts. Each year, plant pathogens cause hundreds of billions of dollars in losses (Fried et al. 2017), and with climate change and global trade, new virulent host-pathogen interactions are emerging with increasing frequency (Anderson et al. 2020). The development of more sustainable agricultural practices will largely hinge on our ability to more effectively predict and prevent the evolution of

virulence in plant pathogens. We need a practical theory of virulence evolution that works for plants.

Here, we use meta-analysis to try to improve our view of the potential usefulness of the Trade-off Hypothesis for plant pathosystems. More concretely, we aim to test the assumption of a direct causal relationship between pathogen accumulation and virulence.

Methods

To assemble a set of relevant studies we conducted a literature search using the various search parameters "plant AND virulence* AND (transmission OR population OR trade off OR fitness effects OR pathogen density OR titer OR replication rate OR aggressiveness)." Literature searches were conducted from 7 October 2020 to 18 February 2021 using Web of Science and Google Scholar. Studies were also identified from the citations of two review papers (Sacristán and García-Arenal 2008, Froissart et al. 2010). To be included in the meta-analysis, a study had to measure both virulence and pathogen accumulation in the same host plants. Additionally, studies had to report means and measures of variance for both variables. By reading the abstracts of studies returned by the literature searches, we identified 210 candidate studies. Of this candidate set, 192 were excluded because they did not meet the criteria for inclusion, leaving 18 suitable studies (bibliography provided in **S3.8**), most of which reported on multiple experiments and thus yielded multiple effect sizes, the total of which was 282 (S2). Further details on the search are presented as a PRISMA flow diagram (Moher et al. 2009) in **Figure 3.3**.

The included studies quantify plant vigor in a variety of ways, specifically, by measuring (i) plant life span, (ii) the extent of diseased tissue, or (iii) the biomass of some part of a plant. Likewise, virulence effects are also expressed in variety of ways, specifically (i) differences between mean values of vigor variables in infected and uninfected plants, (ii) the ratio of vigor values between infected and uninfected plants, (iii) the absolute proportion of diseased tissue, and (iv) categorical ratings of disease severity. The most commonly-used measure of virulence by far is a ratio of biomass in infected versus uninfected plants (253 out of 282 effect sizes), with much emphasis on the mass of reproductive structures such as seeds and inflorescences (228 effect sizes) (**Figure 3.1**).

The study systems also vary; researchers have examined 10 pathogen species, including viruses, fungi, and bacteria, along with 11 host plant species representing six plant families (**Figure 3.1**). But some systems have been studied more than others; indeed, 240 of 282 effect sizes come from studies of *Arabidopsis thaliana*, and 262 effect sizes come from studies of either cucumber mosaic virus or turnip mosaic virus. Hence, our current view of the interactions between plant pathogens and their hosts is strongly biased towards a few model systems.

Wherever possible, experimental effects were taken from the original text and tables. Otherwise, data were extracted from graphs with WebPlotDigitizer (Rohatgi 2020). To make experimental effects comparable across studies, we used the *R* package *metafor* (Viechtbauer 2010) to calculate standardized mean differences. For studies in which virulence effects were expressed as ratios of biomass of infected versus uninfected plants, we calculated the standardized mean difference by dividing the mean by the standard deviation, and we calculated the variance following Hedges (1981) (Hedges 1981). When virulence effects were provided as ratings of disease severity, they were converted into proportional effects by dividing each rating by the

maximum possible rating. In some studies, there was no uninfected control treatment *per se*, but rather, virulence was compared between infections by different pathogen strains, or with different pathogen densities. In these cases, we contrasted virulence levels between the experimental treatment with the lowest and highest levels of pathogen accumulation. For studies where standard errors were used to measure effect dispersion these were converted to standard deviations. For combinability and ease of interpretation, we standardized virulence measures so that larger values always corresponded to higher levels of virulence.

Mixed-effect, multi-level meta-analytic models were fit with *metafor*. We tested for a correlation between standard mean differences in virulence and pathogen accumulation by including the latter as a fixed effect in the model, that is, as a moderator. We also examined several additional fixed effect moderators that we suspected could explain variation across studies: (i) host genotype (tolerant or susceptible), (ii) host age at infection (in days), (iii) the time after inoculation at which pathogen accumulation and virulence were measured (in days), (iv) host vigor variable type (biomass, life span, disease severity), and (v) the publication year of the study. We also included three pairs of nested random effects: (i) plant species within plant family, (ii) pathogen species within pathogen phylum (virus, bacteria, fungus), and (iii) study within lab group. For the study effect, when authors examined multiple plant vigor variables, each was apportioned to a separate factor level; hence, there were 23 study levels from 18 publications.

Our main, "all variables," model included all types of vigor variables, virulence measures, and each of the mentioned fixed and random effects. For some of the fixed effects – namely, host genotype, host age at infection, and the time at which virulence and pathogen accumulation were measured – data were not available for all studies. The main model excluded studies lacking these data. We also fit an "all studies" model in which these effects were omitted, and therefore

all studies could be included. To further our sense of the heterogeneity across studies, we also fit models restricted to each type of vigor variable. In these models, some of the fixed or random effects included in the main model were invariant, and therefore were omitted. See the model specifications in S3 for further details.

For each model, to test for publication bias, which occurs when significant results are more likely to be published than non-significant results, we used a version of Egger's test (Egger et al. 1997), implemented in *metafor*.

Results

By and large, across models, increasing pathogen accumulation maps to increasing virulence (**Table 3.1**). In the main, "all variables" model, based on 71 effect sizes, we found a significant positive correlation between virulence and pathogen accumulation. The effect of pathogen accumulation on virulence was 0.38 standard mean difference (SMD) (± 0.12 se, p-value <<0.001; **Figure 3.2**, **Table 3.2**). Likewise, although diminished in magnitude, the correlation between pathogen accumulation and virulence was positive and significant in the "all studies" model; specifically, across 271 observations, the mean effect of pathogen accumulation was 0.13 SMD (± 0.053 se, p-value = 0.013; **Figure 3.2, Table 3.3**). A positive effect was also estimated in analyzes restricted to studies in which virulence was measured as changes in plant biomass (199 effects sizes; **Table 3.4**). By contrast the effect was insignificant when we looked only at studies which characterized virulence by symptom severity (13 effect sizes; **Table 3.5**), and when we analyzed only studies in which virulence was measured as changes in plant life span, the effect of pathogen accumulation was strongly negative, -1.59 SMD (± 0.63 se, p-value =

0.011; **Table 3.6**), although this was based on only ten effect sizes. With this exception, the Trade-off Hypothesis would seem to hold for plant pathosystems.

Although that is the general trend, studies and pathosystems vary widely. In the "all variables" model, two fixed effect moderators other than pathogen accumulation predict virulence: (i) virulence is reduced by -1.36 SMD (± 0.42 se, p-value = 0.0011) when it is measured as changes in life span, and (ii) virulence declines by -0.41 SMD (± 0.15 se, p-value = 0.0063) with each increasing study year. Moreover, the random effect variance components are considerable: (i) $\boldsymbol{\sigma^2}$ across plant families = 0.058, (ii) $\boldsymbol{\sigma^2}$ across plant species within families = 2.02, (iii) $\boldsymbol{\sigma^2}$ across lab groups = 0.06, (iv) $\boldsymbol{\sigma^2}$ across studies within lab groups = 0.17, (v) $\boldsymbol{\sigma^2}$ across pathogen phyla = 0.058, (vi) $\boldsymbol{\sigma^2}$ across pathogen species within phyla = 1.58. If we constrain each of these random variance components to be zero, it reduces the model fit by 39.74 AICc units. The $\boldsymbol{I^2}$ estimator of the amount of effect size variation that occurs between (as opposed to within) studies is 67%, and after apportioning effect size variation across random effects, there is still a significant amount of residual heterogeneity across studies ($\boldsymbol{Q_E}$=214.8, p-value < 0.0001).

If we look only at studies in which virulence was measured as changes in biomass, increasing the study year has a -0.19 SMD effect on virulence (± 0.04 se, p-value = 0.0001). Also, the estimated effect of tolerant host genotypes on virulence was significant and positive (0.2 SMD; ± 0.08 se, p-value =0.012). This effect had the same sign in the main, "all-variables," model, although in that case it was not significant. Here we should note that an Egger's test indicated significant publication bias in the biomass-only data set (p-value < 0.0001). This was also the case for the model restricted to characterizations of virulence based on symptom severity; Egger's tests on the other models did not indicate significant bias (**Table 3.1**). No fixed effect moderators were

significant in a model restricted to studies of changes in disease severity, and none other than pathogen accumulation was significant in the life-span only model.

In the "all variables" model, there was a high ratio of fixed and random effect moderators to effect sizes: 13 moderator to 71 effect sizes. In the "all studies" model this ratio was less extreme: 10 moderators to 271 effect size. But the total number of levels across categorical random effect variables was 66. The upshot is that our estimates of fixed and random effects were spread thin. The 'study' random effect had 24 levels, which was 12 more than the next most complex random effect, plant species, with 11 levels. To get a sense for the robustness of our inferences, we fit a "simple" version of the "all variables" model in which the random study effect was omitted, summarized in **Table 3.7**. This caused one additional fixed effect to be significant: adding a day to the time post inoculation at which virulence and pathogen accumulation were measured caused a -0.24SMD change in virulence (± 0.09 se, p-value < .0001). But statistically, this model was a worse fit to the data (deltaAICc = 6.86; Likelihood Ratio Test p-value = 0.0015).

Discussion

Our meta-analysis of the empirical research literature suggests that in plant pathosystems, as posited by the Trade-off Hypothesis, there is a general positive link between pathogen accumulation and virulence. That being said, our analysis could potentially be limited by our search terms, even though we attempted to be as comprehensive and inclusive as possible. Our analysis also foregrounds that much of what we know about the relationship between pathogen accumulation and virulence is based on a few model systems, in particular, infections of *Arabidopsis thaliana* by cucumber mosaic virus and turnip mosaic virus. Moreover, what

happens in those model systems is not necessarily what happens in other systems; in fact, we found a wide variety of pathogen effects on their hosts. The optimization of general life history trade-offs in pathogen populations is only part of what drives the evolution of virulence.

Two seemingly aberrant statistical relationships warrant special consideration. First, when we analyzed the subset of the studies for which virulence was measured as changes in life span, we found that pathogen accumulation had a strong negative effect. At first glance, this seems counter-intuitive, and it could be a sampling artifact; with only ten effect sizes, there is a high potential of mistaking statistical noise for signal. It could also be explained by reversing the arrow of causation; a negative relationship between pathogen accumulation and virulence could reflect that pathogens tend to have more time to accumulate when infections are less virulent and host live longer (O'Keefe and Antonovics 2002, Ebert et al. 2004, Montes et al. 2020). If this were the case, it would be contra the Trade-off Hypothesis. But another possibility is that infection by a pathogen increases host life span while reducing overall reproductive fitness. In other words, physiological trade-offs in hosts mask demographic trade-offs in pathogen populations. Indeed, the viral pathogens most strongly represented in the meta-data set can in some cases sterilize their hosts (Pagán et al. 2007, Vijayan et al. 2017, Montes et al. 2019, 2020) which may redirect resources away from reproduction and toward survival (Lafferty and Kuris 2009, Vijayan et al. 2017).

We found a second seemingly aberrant relationship when we restricted our analysis to studies in which virulence was characterized by changes in biomass. In that case, we found that purportedly tolerant host genotypes tended to exhibit more pronounced signs of virulence – not

what one would expect. This could also be explained as a statistical artifact, or, as for the anomalous effects of pathogen accumulation on life span, it could also be interpreted as evidence of pathogen-induced physiological trade-offs. The lion's share of studies that view virulence as changes in plant biomass focus on changes in seed or inflorescence biomass. It could be that the plant genotypes classified as tolerant maintain vegetative vigor at the cost of decreased seed production.

These aberrant inferences drive home something that has been noted by many previous authors, namely, that empirical characterizations of virulence – such as differences in biomass or ratings of disease severity – are only indirect reflections of the standard theoretical concept of virulence as the excess death caused by infection (Read 1994, Alizon et al. 2009, 2015, Pagan and Garcia-Arenal 2020). For evolutionary studies, that theoretical concept might also be too reductive, especially if virulence involves trade-offs between longevity and fecundity (Schürch and Roy 2004, Pagán et al. 2007, Sacristán and García-Arenal 2008). Concretely, if infected hosts are less fecund, and that causes a demographic decline, pathogen transmission rates and meta-population-level fitness should be adversely affected. Hence, as for reductions in longevity, reductions in fecundity should also select against high virulence. Regardless, for the theory to be applicable, the empirical measure of virulence needs to be sufficiently integrative to approximate its fitness effects on a pathogen population. To reiterate, when we look across all of the published research, we find that by and large, there is a positive correlation between pathogen accumulation and virulence, however it is measured, which suggests that relatively simple measures of virulence can be useful. But when that correlation breaks down or reverses sign, it could indicate that virulence measures are too simple.

Since published studies have mostly focused on a few model systems, we were unable to explore the effects of several additional factors that could affect the relationship between pathogen accumulation and virulence. For example, the ecological apparency and longevity of host plants could affect virulence evolution (Choo et al. 2003), but only relatively short-lived annual species have been studied. As another example, the phenological stage of the host at the time of infection can influence virulence (Bingham et al. 2009, Pagan and Garcia-Arenal 2020), but we were unable to include this as a moderator, as it varied little across studies. Furthermore, pathogen loads can fluctuate over the infection period and our single-value measures of accumulation miss much of this variation. As more empirical research accumulates, the scope for more sophisticated meta-analysis will expand.

At the onset, we suspected that in plants a preponderance of tolerant genotypes (Baucom and De Roode 2011), and immunopathological responses (Maekawa et al. 2011) might be sufficient to erase any sign of a general positive relationship between pathogen accumulation and virulence. Although that does not appear to be the case, those factors might explain some of the wide variation we observed across studies and systems. Indeed, although the extent of immunopathology was not characterized in any of the examined studies, host genotype was one of the strongest predictors of virulence. The wide variety of virulence effects could also be telling us that some of the observed levels of virulence are non-adaptive, or are adaptive only in un-examined ecological contexts. Most theoretical investigations of virulence evolution are based on evolutionary invasion analyses that predict long-term evolutionary equilibria, but it can take a long time for populations to reach such states and in non-equilibrium conditions, alleles

that increase or decrease virulence can be under positive selection (Day and Gandon 2007, Parker et al. 2012, Vanhove et al. 2019). And there have been multiple theoretical demonstrations of how competition between pathogen strains can cause the evolution of virulence above the level that would optimize fitness in the absence of competition (Frank 1996, Buckling and Brockhurst 2008, Leggett et al. 2013). Life history optimization in a single pathogen population is only part of the story.

Conclusion

In simple systems near equilibrium, virulence reduces the fitness of hosts and pathogens alike; alleles that increase virulence should be selected against. And yet many pathogens are highly virulent. The evolution of such virulence tends to be explained by assuming a hard-and-fast trade-off between pathogen accumulation, which governs instantaneous transmission efficiency, and host health. Although there had been some doubt, here we show that such a trade-off does appear to apply to plant pathosystems. We also show considerable variation in virulence effects, which may reflect the preponderance of plant immunopathology and the wide range of tolerance phenotypes in plant populations, as well as the non-equilibrium status and complex ecology of many plant pathosystems. The Trade-off Hypothesis is something to build on. More empirical studies are highly welcomed, especially those comparing several strains of pathogen in a single host genotype with simultaneous measures of pathogen accumulation, transmission rates, and virulence taken several times throughout multiple host generations. Repeating such studies across pathosystems would provide great insight into the extent of how generalizable the trade-off hypothesis truly is.

Acknowledgements

This work was supported by the Alabama Agricultural Experiment Station (AAES) Hatch Program (L.D.F. and N.B.H.).

References – Chapter III

Acevedo, M. A., F. P. Dillemuth, A. J. Flick, M. J. Faldyn, and B. D. Elderd. **2019**. Virulence-driven trade-offs in disease transmission: A meta-analysis*. Evolution (N. Y). 73: 636–647.

Alizon, S., A. Hurford, N. Mideo, and M. Van Baalen. **2009**. Virulence evolution and the trade-off hypothesis: History, current state of affairs and the future. J. Evol. Biol. 22: 245–259.

Alizon, S., Y. Michalakis, S. Alizon, and Y. Michalakis. **2015**. Adaptive virulence evolution : the good old fitness-based approach To cite this version : HAL Id : hal-01567907 Adaptive virulence evolution : the good old fitness-based approach.

Anderson, K., D. P. Bebber, K. A. Brauman, N. J. Cunniffe, N. V Fedoroff, C. Finegold, K. A. Garrett, A. Gilligan, C. M. Jones, M. D. Martin, K. Macdonald, P. Neenan, A. Records, D. G. Schmale, L. Tateosian, and Q. Wei. **2021**. The persistent threat of emerging plant disease pandemics to global food security. Proc. Natl. Acad. Sci. U. S. A. 118.

Anderson, R., P. E. Bayer, and D. Edwards. **2020**. Climate change and the need for agricultural adaptation. Curr. Opin. Plant Biol. 56: 197–202.

Anderson, R. M., and R. M. May. **1982**. Coevolution of Hosts and Parasites. Parasitology. 85: 411–426.

Baucom, R. S., and J. C. De Roode. **2011**. Ecological immunology and tolerance in plants and animals. Funct. Ecol. 25: 18–28.

Bingham, I. J., D. R. Walters, M. J. Foulkes, and N. D. Paveley. **2009**. Crop traits and the

tolerance of wheat and barley to foliar disease. Ann. Appl. Biol. 154: 159–173.

Buckling, A., and M. A. Brockhurst. **2008**. Kin selection and the evolution of virulence. Heredity (Edinb). 100: 484–488.

Bull, J. J. 1994. Evolution: An international journal of organic evolution. Nature. 161: 162–163.

Bull, J. J., and A. S. Lauring. **2014**. Theory and Empiricism in Virulence Evolution. PLoS Pathog. 10: 1–3.

Choo, K., P. D. Williams, and T. Day. **2003**. Host mortality, predation and the evolution of parasite virulence. Ecol. Lett. 6: 310–315.

Cressler, C. E., D. V. McLeod, C. Rozins, J. Van Den Hoogen, and T. Day. **2016**. The adaptive evolution of virulence: A review of theoretical predictions and empirical tests. Parasitology. 143: 915–930.

D'arcy, C. J., D. M. Eastburn, and G. L. Schumann. **2001**. Illustrated Glossary of Plant Pathology.

Day, T., and S. Gandon. **2007**. Applying population-genetic models in theoretical evolutionary epidemiology. Ecol. Lett. 10: 876–888.

Ebert, D., H. J. Carius, T. Little, and E. Decaestecker. **2004**. The evolution of virulence when parasites cause host castration and gigantism. Am. Nat. 164.

Ebert, D., and K. L. Mangin. **1997**. The influence of host demography on the evolution of virulence of a microsporidian gut parasite. Evolution (N. Y). 51: 1828–1837.

Egger, M., G. D. Smith, M. Schneider, and C. Minder. **1997**. Bias in meta-analysis detected by a simple, graphical test. Br. Med. J. 315: 629–634.

Frank, S. A. 1996. Models of parasite virulence. Q. Rev. Biol. 71: 37–78.

Fried, G., B. Chauvel, P. Reynaud, and I. Sache. **2017**. Impact of Biological Invasions on

Ecosystem Services. Impact Biol. Invasions Ecosyst. Serv.

Froissart, R., J. Doumayrou, F. Vuillaume, S. Alizon, and Y. Michalakis. **2010**. The virulence-transmission trade-off in vector-borne plant viruses: A review of (non-)existing studies. Philos. Trans. R. Soc. B Biol. Sci. 365: 1907–1918.

Graham, A. L., J. E. Allen, and A. F. Read. **2005**. Evolutionary causes and consequences of immunopathology. Annu. Rev. Ecol. Evol. Syst. 36: 373–397.

Hedges, L. V. 1981. Distribution Theory for Glass's Estimator of Effect size and Related Estimators. J. Educ. Stat. 6: 107–128.

Jensen, K. H., T. Little, A. Skorping, and D. Ebert. **2006**. Empirical support for optimal virulence in a castrating parasite. PLoS Biol. 4: 1265–1269.

Lafferty, K. D., and A. M. Kuris. **2009**. Parasitic castration: the evolution and ecology of body snatchers. Trends Parasitol. 25: 564–572.

Lam, E., N. Kato, and M. Lawton. **2001**. Programmed cell death, mitochondria and the plant hypersensitive response. Nature. 411: 848–853.

Leggett, H. C., A. Buckling, G. H. Long, and M. Boots. **2013**. Generalism and the evolution of parasite virulence. Trends Ecol. Evol. 28: 592–596.

Lipsitch, M., and E. R. Moxon. **1997**. Virulence and transmissibility of pathogens: What is the relationship? Trends Microbiol. 5: 31–37.

Mackinnon, M. J., and A. F. Read. **2004**. Virulence in malaria: An evolutionary viewpoint. Philos. Trans. R. Soc. B Biol. Sci. 359: 965–986.

Maekawa, T., T. A. Kufer, and P. Schulze-Lefert. **2011**. NLR functions in plant and animal immune systems: So far and yet so close. Nat. Immunol. 12: 818–826.

Miller, M. R., A. White, and M. Boots. **2006**. The Evolution of Parasites in Response to

Tolerance in Their Hosts : The Good , the Bad , and Apparent Commensalism. 60: 945–956.

Moher, D., A. Liberati, J. Tetzlaff, D. G. Altman, D. Altman, G. Antes, D. Atkins, V. Barbour, N. Barrowman, J. A. Berlin, J. Clark, M. Clarke, D. Cook, R. D'Amico, J. J. Deeks, P. J. Devereaux, K. Dickersin, M. Egger, E. Ernst, P. C. Gøtzsche, J. Grimshaw, G. Guyatt, J. Higgins, J. P. A. Ioannidis, J. Kleijnen, T. Lang, N. Magrini, D. McNamee, L. Moja, C. Mulrow, M. Napoli, A. Oxman, B. Pham, D. Rennie, M. Sampson, K. F. Schulz, P. G. Shekelle, D. Tovey, and P. Tugwell. **2009**. Preferred reporting items for systematic reviews and meta-analyses: The PRISMA statement. PLoS Med. 6.

Montes, N., C. Alonso-Blanco, and F. García-Arenal. **2019**. Cucumber mosaic virus infection as a potential selective pressure on arabidopsis thaliana populations. PLoS Pathog. 15: 1–24.

Montes, N., V. Vijayan, and I. Pagan. **2020**. Trade-offs between host tolerances to different pathogens in plant-virus interactions. Virus Evol. 6: 1–12.

O'Keefe, K. J., and J. Antonovics. **2002**. Playing by different rules: The evolution of virulence in sterilizing pathogens. Am. Nat. 159: 597–605.

Pagán, I., C. Alonso-Blanco, and F. García-Arenal. **2007**. The relationship of within-host multiplication and virulence in a plant-virus system. PLoS One. 2.

Pagan, I., and F. Garcia-Arenal. **2020**. Tolerance of Plants to Pathogens: A Unifying View. Annu. Rev. Phytopathol. 58: 77–96.

Parker, J. K., J. C. Havird, and L. De La Fuente. **2012**. Differentiation of Xylella fastidiosa strains via multilocus sequence analysis of environmentally mediated genes (MLSA-E). Appl. Environ. Microbiol. 78: 1385–1396.

R Core Team, R. F. for S. C. 2019. R: A Language and Environment.

Råberg, L. 2014. How to Live with the Enemy: Understanding Tolerance to Parasites. PLoS Biol. 12.

Read, A. F. 1994. The evolution of virulence. Trends Microbiol. 2: 73–76.

Rohatgi, A. 2020. WebPlotDigitizer.

Sacristán, S., and F. García-Arenal. **2008**. The evolution of virulence and pathogenicity in plant pathogen populations. Mol. Plant Pathol. 9: 369–384.

Schürch, S., and B. A. Roy. **2004**. Comparing single- vs. mixed-genotype infections of Mycosphaerella graminicola on wheat: Effects on pathogen virulence and host tolerance. Evol. Ecol. 18: 1–14.

Vanhove, M., A. C. Retchless, A. Sicard, A. Rieux, H. D. Coletta-Filho, L. De La Fuente, D. C. Stenger, and R. P. P. Almeida. **2019**. Genomic diversity and recombination among Xylella fastidiosa subspecies. Appl. Environ. Microbiol. 85.

Viechtbauer, W. 2010. Conducting meta-analyses in R with the metafor. J. Stat. Softw. 36: 1–48.

Vijayan, V., S. López-González, F. Sánchez, F. Ponz, and I. Pagán. **2017**. Virulence evolution of a sterilizing plant virus: Tuning multiplication and resource exploitation. Virus Evol. 3: 1–11.

Figures and Tables – Chapter III

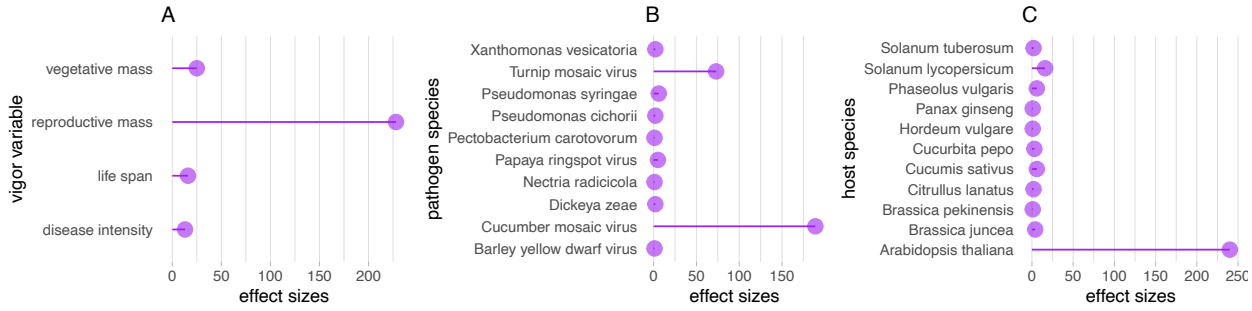

Figure 3.1: Study System Variation. Lollipop plots showing the number of effect sizes from studies with (A) different measures of host plant vigor, (B) different host plant species, and (C) different pathogen species. *Interpretation*: Most studies have measured virulence as changes in plant biomass and have examined infections of *Arabidopsis thaliana* by either cucumber mosaic virus or turnip mosaic virus.

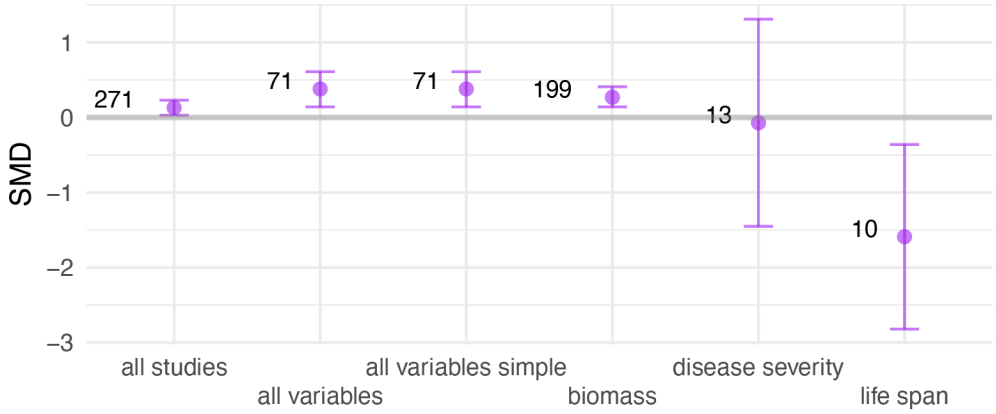

Figure 3.2: Effect of Pathogen Accumulation on Virulence. Shown are the effects in standard mean differences (SMD) of pathogen accumulation on virulence estimated from each of the models described in the main text. Whiskers show confidence intervals. The number beside each point is the number of effect sizes from which it was estimated. The "all studies" model excludes the host-plant-age and infection-duration covariates. The "all variables" model excludes studies without data for host-plant-age and infection-duration. The "all variables simple" model is like the previous except that it has a simpler set of random effects, specifically, it does not

include a study effect nested within the random lab group effect. The remaining models are of subsets of the data, each restricted to a particular measure of host plant vigor. *Interpretation*: With the exception of the model restricted to studies of virulence measured as changes in life span, there is a significant positive relationship between pathogen accumulation and virulence.

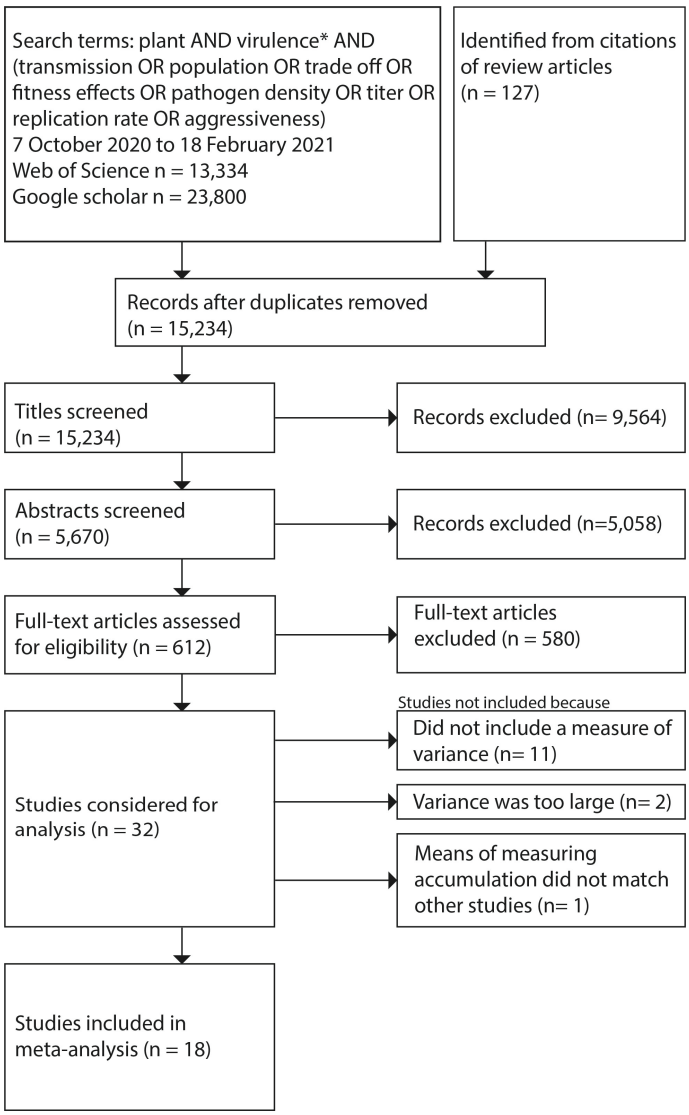

(Moher et al 2009)

Figure 3.3: Prisma Flow Chart. Documents the step-by-step process of the literature review

Table 3.1: Estimates Effects of Pathogen Accumulation on Virulence. Each row gives (1) the estimated effect (SMD) for a model, along with (2) its p-value (p.val), (3) upper bound of the 95% confidence interval (ci.ub), (4) lower bound of the 95% confidence interval (ci.lb), (5) the number of effect sizes it was estimated from (k), (6) the number of fixed effect coefficients in the model (p), (7) the model's log likelihood (logLik), (8) AICc score, (9) the I^2 estimator of proportion of effect size variation across versus within studies, and (10) the p-value of Egger's test for publication bias (pub.bias). All figures were rounded to two significant digits.

model	SMD	p.val	ci.ub	ci.lb	se	k	p	logLik	AICc	i2	pub.bias
all studies	0.13	0.01	0.23	0.03	0.05	271	6	-720.27	1465.75	0.85	0.27
all variables	0.38	0	0.61	0.14	0.12	71	7	-105.1	242.58	0.67	0.21
all variables simple	0.38	0	0.61	0.14	0.12	71	7	-107.91	245.2	0.67	0.21
life span	-1.59	0.01	-0.36	-2.82	0.63	10	3	-23.47	71.93	0.89	0.73
disease severity	-0.07	0.92	1.31	-1.45	0.7	13	4	-50.67	137.74	0.92	0.01
biomass	0.27	0	0.41	0.14	0.07	199	5	-471.42	966.26	0.8	0

Table 3.2. Summary of "All Variables" Model.

	beta	se	ci.lb	ci.ub	p.val
intercept	830.04	304.36	233.51	1426.57	0.01
pathogen accumulation	0.38	0.12	0.14	0.61	0
host genotype: tolerant	0.16	0.26	-0.36	0.67	0.55
vigor variable: life_span	-1.36	0.42	-2.18	-0.54	0
days post inoculation	-0.2	0.15	-0.49	0.08	0.16
study year	-0.41	0.15	-0.7	-0.12	0.01
age at infection	-0.19	0.24	-0.66	0.27	0.42

Table 3.3. Summary of "All Studies" Model.

	beta	se	ci.lb	ci.ub	p.val
intercept	136.54	81.05	-22.31	295.4	0.09
pathogen accumulation	0.13	0.05	0.03	0.23	0.01
vigor_variable-life_span	-1.58	0.48	-2.53	-0.64	0
vigor_variable-severity_area	-0.73	10.59	-21.48	20.03	0.95
vigor_variable-severity_percentage	11.32	9.43	-7.15	29.79	0.23
study_year	-0.07	0.04	-0.15	0.01	0.09

Table 3.4. Summary of Model Restricted to Measures of Biomass.

	beta	se	ci.lb	ci.ub	p.val
intercept	379.61	72.1	238.3	520.92	0

pathogen accumulation	0.27	0.07	0.14	0.41	0
host genotype: tolerant	0.2	0.08	0.04	0.36	0.01
study year	-0.19	0.04	-0.26	-0.12	0
age at infection	0.03	0.15	-0.27	0.33	0.84

Table 3.5. Summary of Model Restricted to Measures of Disease Severity.

	beta	se	ci.lb	ci.ub	p.val
intercept	1651.33	4255.13	-6688.58	9991.23	0.7
pathogen accumulation	-0.07	0.7	-1.45	1.31	0.92
study year	-0.82	2.12	-4.98	3.33	0.7
age at infection	0.89	1.37	-1.79	3.57	0.51

Table 3.6. Summary of Model Restricted to Measures of Life Span.

	beta	se	ci.lb	ci.ub	p.val
intercept	-1.7	1.52	-4.69	1.29	0.26
pathogen accumulation	-1.59	0.63	-2.82	-0.36	0.01
host genotype: tolerant	0.79	0.41	-0.02	1.6	0.06

Table 3.7. Summary of "All Variables Simple" Model.

	beta	se	cilb	ciub	pval
intercept	928.12	205.39	525.56	1330.68	0
pathogen accumulation	0.38	0.12	0.14	0.61	0
host genotype: tolerant	0.15	0.26	-0.36	0.67	0.56
vigor variable: life_span	-1.2	0.17	-1.53	-0.88	0
days post inoculation	-0.24	0.09	-0.41	-0.07	0
study year	-0.46	0.1	-0.65	-0.26	0
age at infection	-0.24	0.2	-0.63	0.14	0.22

S3.8 Studies Used in the Meta-Analysis

1. Ahn IP, Lee YH. A viral double-stranded RNA up regulates the fungal virulence of Nectria radicicola. Mol Plant-Microbe Interact. 2001;14(4):496–507. doi: 10.1094/MPMI.2001.14.4.496
2. Cobos A, Montes N, López-Herranz M, Gil-Valle M, Pagán I. Within-Host Multiplication and Speed of Colonization as Infection Traits Associated with Plant Virus Vertical Transmission. J Virol. 2019;93(23). doi: 10.1128/jvi.01078-19
3. Felipe V, Romero AM, Montecchia MS, Vojnov AA, Bianco MI, Yaryura PM. Xanthomonas vesicatoria virulence factors involved in early stages of bacterial spot development in tomato. Plant Pathol. 2018;67(9):1936–43. doi: 10.1111/ppa.12905
4. Hu M, Li J, Chen R, Li W, Feng L, Shi L, et al. Dickeya zeae strains isolated from rice, banana and clivia rot plants show great virulence differentials. BMC Microbiol. 2018;18(1):1–16. doi: 10.1186/s12866-018-1300-y
5. Hwang IS, Lee HM, Oh EJ, Lee S, Heu S, Oh CS. Plasmid composition and the chpG gene determine the virulence level of Clavibacter capsici natural isolates in pepper. Mol Plant Pathol. 2020;21(6):808–19. doi: 10.1111/mpp.12932
6. Jiménez-Fernández D, Montes-Borrego M, Jiménez-Díaz RM, Navas-Cortés JA, Landa BB. In planta and soil quantification of Fusarium oxysporum f. sp. ciceris and evaluation of fusarium wilt resistance in chickpea with a newly developed quantitative polymerase chain reaction assay. Vol. 101, Phytopathology. 2011. p. 250–62. doi: 10.1094/PHYTO-07-10-0190
7. Marchetto KM, Power AG. Coinfection timing drives host population dynamics through changes in virulence. Am Nat. 2018;191(2):173–83. doi: 10.1086/695316
8. Moyano L, Carrau A, Petrocelli S, Kraiselburd I, Gärtner W, Orellano EG. Bacteriophytochromes from Pseudomonas syringae pv. tomato DC3000 modulate the early stages of plant colonization during bacterial speck disease. Eur J Plant Pathol. 2020;156(3):695–712. doi: 10.1007/s10658-019-01918-5
9. Moleleki LN, Pretorius RG, Tanui CK, Mosina G, Theron J. A quorum sensing-defective mutant of Pectobacterium carotovorum ssp. brasiliense 1692 is attenuated in virulence and unable to occlude xylem tissue of susceptible potato plant stems. Mol Plant Pathol.

2017;18(1):32–44. doi: 10.1111/mpp.12372

10. Montes N, Pagán I. Light intensity modulates the efficiency of virus seed transmission through modifications of plant tolerance. Plants. 2019;8(9). doi: 10.3390/plants8090304
11. Montes N, Vijayan V, Pagan I. Trade-offs between host tolerances to different pathogens in plant-virus interactions. Virus Evol. 2020;6(1):1–12. doi: 10.1093/VE/VEAA019
12. Pacheco DA, Rezende JAM, Piedade SM de S. Biomass, virus concentration, and symptomatology of cucurbits infected by mild and severe strains of Papaya ringspot virus. Sci Agric. 2003;60(4):691–8. doi: 10.1590/s0103-90162003000400013
13. Pagán I, Alonso-Blanco C, García-Arenal F. The relationship of within-host multiplication and virulence in a plant-virus system. PLoS One. 2007;2(8). doi: 10.1371/journal.pone.0000786
14. Pagán I, Montes N, Milgroom MG, García-Arenal F. Vertical Transmission Selects for Reduced Virulence in a Plant Virus and for Increased Resistance in the Host. PLoS Pathog. 2014;10(7):23–5. doi: 10.1371/journal.ppat.1004293
15. Rajendran DK, Park E, Nagendran R, Hung NB, Cho BK, Kim KH, et al. Visual analysis for detection and quantification of Pseudomonas cichorii disease severity in tomato plants. Plant Pathol J. 2016;32(4):300–10. doi: 10.5423/PPJ.OA.01.2016.0032
16. Ritchie F, Bain R, Mcquilken M. Survival of Sclerotia of Rhizoctonia solani AG3PT and Effect of Soil-Borne Inoculum Density on Disease Development on Potato. J Phytopathol. 2013;161(3):180–9. doi: 10.1111/jph.12052
17. Sacristán S, Fraile A, Malpica JM, García-Arenal F. An analysis of host adaptation and its relationship with virulence in Cucumber mosaic virus. Phytopathology. 2005;95(7):827–33. doi: 10.1094/PHYTO-95-0827
18. Vijayan V, López-González S, Sánchez F, Ponz F, Pagán I. Virulence evolution of a sterilizing plant virus: Tuning multiplication and resource exploitation. Virus Evol. 2017;3(2):1–11. doi: 10.1093/ve/vex033